

MODELING AND SIMULATION OF PARALLEL D-STATCOMS  
WITH FULL-WAVE RECTIFIERS

A Thesis  
presented to  
the Faculty of California Polytechnic State University,  
San Luis Obispo

In Partial Fulfillment  
of the Requirements for the Degree  
Master of Science in Electrical Engineering

by  
Jason Brinsfield

May 2014

© 2014

Jason Brinsfield

ALL RIGHTS RESERVED

## COMMITTEE MEMBERSHIP

TITLE: Modeling and Simulation of Parallel D-STATCOMs with Full-Wave Rectifiers

AUTHOR: Jason Brinsfield

DATE SUBMITTED: May 2014

COMMITTEE CHAIR: Dr. Taufik, Professor  
Electrical Engineering Department

COMMITTEE MEMBER: Dr. Ali Shaban, Professor  
Electrical Engineering Department

COMMITTEE MEMBER: Dr. Ahmad Nafisi, Professor  
Electrical Engineering Department

## ABSTRACT

### Modeling and Simulation of Parallel D-STATCOMs with Full-Wave Rectifiers

Jason Brinsfield

In recent years, both a significant increase in electrical demand and a large influx of intermittent renewable energy sources have put a considerable stress on the nation's electrical grid. Conventional power flow control techniques such as capacitor banks and tap-changing transformers are incapable of adequately handling the rapid fluctuations in power supply and demand that today's grid experiences. Flexible AC Transmission System (FACTS) controllers are a practical way to compensate for such rapid power fluctuations. One type of shunt FACTS controller is the Static Synchronous Compensator (STATCOM), which uses fully controllable switches to source or sink reactive power to a point on the grid, thus reducing voltage fluctuations due to load changes. The purpose of this thesis is to model and simulate the operation of two Distribution STATCOMs (D-STATCOMs) operating on the same point on the grid. These D-STATCOMs also utilize parallel full-wave rectifiers that directly connect the ac grid to the dc capacitor of the D-STATCOMs. Parameters such as power loss, reaction time, stability, and THD are measured for several test scenarios. Results from this thesis show that two D-STATCOMs operating on the same point can be stable and effective under a wide range of conditions. This thesis also concludes that the inclusion of parallel rectifiers with the D-STATCOMs results in no performance improvement of the D-STATCOMs.

## ACKNOWLEDGMENTS

Firstly, I would like to thank my parents for all the support they have given me. They are responsible for sparking my initial interest in electrical engineering from a young age, and they have supported me in so many ways throughout my college career. I would not be the person I am today without their guidance and support.

I would also like to thank Dr. Taufik for his wonderful job advising me throughout this thesis. His knowledge and passion for power electronics is a tremendous asset to his students. Furthermore, his ability to take on the challenges and time commitments of advising, teaching, and research, is superhuman.

Disclaimer:

SDG&E does not endorse or accept the conclusions or results of this study.

## TABLE OF CONTENTS

LIST OF TABLES .....	ix
LIST OF FIGURES .....	x
1 Introduction.....	1
1.1 Sustainability.....	1
1.2 Increased Electrical Energy Consumption.....	3
1.3 Impact on Power Quality .....	4
1.4 FACTS Controllers .....	5
2 Background.....	7
2.1 Power Flow in Transmission Lines.....	7
2.2 Power Flow and FACTS Devices .....	10
2.2.1 Series Controllers .....	11
2.2.2 Shunt Controllers.....	12
2.2.2.1 Static Var Compensator.....	12
2.2.2.2 STATCOMs .....	13
2.3 Thesis Objective.....	16
3 Design Requirements .....	18
3.1 Hardware Requirements.....	19
3.2 Control Requirements .....	19
3.3 System Requirements.....	20
4 PSCAD Model and Simulation.....	21
4.1 System Components .....	21

4.1.1	Grid Voltage and Impedance .....	22
4.1.2	Load .....	22
4.1.3	Transformers .....	23
4.1.4	Capacitors .....	24
4.1.5	Three-Phase Full-Wave Rectifier .....	24
4.2	The D-STATCOM Module .....	25
4.2.1	SPWM Generator .....	26
4.2.2	Six-Pulse IGBT Gate Drive .....	29
4.2.3	Six-Pulse IGBT Bridge .....	30
4.2.4	Output Filtering .....	35
4.2.5	Internal Power Measurement.....	37
4.3	Control Module .....	38
4.3.1	DC Voltage Regulator .....	38
4.3.2	AC Voltage Regulator .....	40
4.4	Control Module Tuning .....	42
4.4.1	Measurement Smoothing Time Constants .....	43
4.4.2	AC Voltage Regulator Tuning .....	46
4.4.3	DC Voltage Regulator Tuning .....	50
5	Testing and Results .....	55
5.1	Full Load With No Regulation .....	55
5.2	Single D-STATCOM Operation .....	56
5.2.1	Single Operation without Parallel Rectifier .....	57
5.2.2	Single Operation with Parallel Rectifier .....	60

5.2.3	Power Loss for Single D-STATCOM .....	65
5.3	Synchronous Dual D-STATCOM Operation Without Initial Load.....	68
5.3.1	Synchronous Operation Without Parallel Rectifier .....	68
5.3.2	Synchronous Operation With Parallel Rectifier .....	71
5.3.3	Synchronous Operation With Parallel Rectifier and Light Load .....	72
5.4	Asynchronous D-STATCOM Operation .....	74
5.5	Asynchronous D-STATCOM Operation With Initial Load .....	77
5.5.1	Asynchronous Operation with Full Initial Load.....	78
5.5.2	Asynchronous Operation With Light Initial Load .....	81
6	Conclusion .....	84
6.1	Future Work.....	85
6.1.1	Alternate Control Schemes for the DC and AC Voltage Regulators ...	85
6.1.2	Integration of D-STATCOM Capabilities into Grid-Tie Inverters .....	85
	Bibliography .....	87



## LIST OF TABLES

Table 4.1 Selected AC Voltage Regulator Tuning Coefficients and Measurements.....	48
Table 4.2 Selected DC Voltage Regulator Tuning Coefficients and Measurements.....	54
Table 5.1 Measured Values, Full Load, No Regulation .....	55
Table 5.2 Measured Values, Single Operation without Parallel Rectifier .....	57
Table 5.3 Measured Values, Single Operation with Parallel Rectifier .....	61
Table 5.4 Measured Values, Power Loss for Single D-STATCOM.....	65
Table 5.5 $\frac{P_{Loss}}{Q_{supplied}}$ for Single D-STATCOM.....	66
Table 5.6 Measured Values, Synchronous Operation Without Parallel Rectifier .....	69
Table 5.7 Measured Values, Synchronous Operation With Parallel Rectifier .....	71
Table 5.8 Measured Values, Synchronous Operation With Parallel Rectifier and Light Load.....	73
Table 5.9 Measured Values, Asynchronous D-STATCOM Operation With Full Load ..	75
Table 5.10 Measured Values, Asynchronous Operation With Full Initial Load .....	78
Table 5.11 Measured Values, Asynchronous Operation With Light Load.....	81

## LIST OF FIGURES

Figure 1.1 Global Renewable Energy Capacity [2] .....	2
Figure 1.2 U.S. Installed Solar Capacity and Yearly Generation [2] .....	2
Figure 1.3 Per Capita Energy Consumption in China and Worldwide [4] .....	3
Figure 1.4 Large Scale PV Output on Cloudy (Left) and Clear (Right) Days [6] .....	4
Figure 1.5 Typical STATCOM Application [7] .....	6
Figure 2.1 Two-Bus System .....	7
Figure 2.2 Series Capacitor in Two-Bus System .....	8
Figure 2.3 Switched Shunt Capacitor .....	9
Figure 2.4 Thyristor-Controlled Series Capacitor .....	11
Figure 2.5 Reactance vs. Firing Angle for TCSC [16] .....	12
Figure 2.6 Components of a Static Var Compensator [14].....	13
Figure 2.7 I-V Characteristics for SVC (Left) and STATCOM (Right) [17].....	14
Figure 2.8 Simplified STATCOM Schematic .....	15
Figure 2.9 Parallel STATCOM System Overview .....	16
Figure 3.1 RTDS System Racks [24].....	18
Figure 4.1 PSCAD Parallel D-STATCOM System Top Level Schematic.....	21
Figure 4.2 Three-Phase Full-Wave Rectifier .....	24
Figure 4.3 D-STATCOM Module .....	25
Figure 4.4 SPWM Generator .....	26
Figure 4.5 RMS Output Magnitude vs. Modulation Index [29] .....	28
Figure 4.6 SPWM Reference and Carrier Waveforms (top) and PWM Waveform (bottom).....	29

Figure 4.7 Six-Pulse IGBT Gate Drive .....	30
Figure 4.8 Six-Pulse IGBT Bridge Schematic .....	31
Figure 4.9 V-I Characteristic for IGBT in PSCAD .....	32
Figure 4.10 Parameters Used for IGBT .....	33
Figure 4.11 V-I Characteristic for Diode in PSCAD .....	34
Figure 4.12 Parameters used for Diode.....	34
Figure 4.13 Output Filter for D-STATCOM .....	35
Figure 4.14 Output Filter Frequency Response .....	36
Figure 4.15 Input and Output Waveforms for Output Filter.....	37
Figure 4.16 Internal Power Measurement Implementation .....	38
Figure 4.17 DC Voltage Regulator Diagram .....	40
Figure 4.18 AC Voltage Regulator Diagram .....	42
Figure 4.19 Reactive Power Measurement Signal with Various Smoothing Time Constants .....	45
Figure 4.20 Unfiltered (top) vs. Filtered (bottom) DC Voltage Signals .....	46
Figure 4.21 PCC Voltage and SPWM Magnitude, Case 1 (0.5 seconds per x- division) .....	48
Figure 4.22 PCC Voltage and SPWM Magnitude, Case 2 (0.5 seconds per x- division) .....	49
Figure 4.23 DC Voltage Response For $K_{p1} = 40$ and $\tau_{i1} = 0.25$ .....	51
Figure 4.24 DC Voltage Regulator Stage 1 Output vs. Stage 2 Error .....	52
Figure 4.25 DC Voltage Response Without Integral Limit .....	53
Figure 4.26 DC Voltage Response with Integral Limit .....	53

Figure 5.1 PCC Voltage, Full Load, No Regulation .....	56
Figure 5.2 PCC Voltage, Single Operation without Parallel Rectifier .....	58
Figure 5.3 Inrush Current, Single Operation without Parallel Rectifier .....	59
Figure 5.4 AC Inrush Current, Single Operation with Parallel Rectifier.....	62
Figure 5.5 PCC Voltage, Single Operation with Parallel Rectifier .....	62
Figure 5.6 PCC Inrush Voltage, Single Operation with and without Parallel Rectifier ...	63
Figure 5.7 DC Ripple Voltage, Single Operation without Parallel Rectifier.....	64
Figure 5.8 DC Ripple Voltage, Single Operation with Parallel Rectifier.....	65
Figure 5.9 $P_{\text{loss}}$ vs. $Q_{\text{supplied}}$ .....	66
Figure 5.10 $\frac{P_{\text{Loss}}}{Q_{\text{Supplied}}}$ vs. $Q_{\text{supplied}}$ .....	67
Figure 5.11 PCC Voltage Waveform With Single STATCOM Online .....	68
Figure 5.12 PCC Voltage, Synchronous Operation Without Parallel Rectifier.....	70
Figure 5.13 PCC Voltage, Synchronous Operation With Parallel Rectifier.....	71
Figure 5.14 PCC Inrush Voltage, Synchronous Operation With and Without Parallel Rectifier.....	72
Figure 5.15 PCC Voltage, Synchronous Operation With Parallel Rectifier and Light Load .....	73
Figure 5.16 PCC Voltage, Asynchronous Operation With Full Load .....	75
Figure 5.17 Real and Reactive Power Transfer, Asynchronous Operation With Full Load .....	77
Figure 5.18 PCC Voltage, Asynchronous Operation With Full Initial Load.....	79
Figure 5.19 Real and Reactive Power Transfer, Asynchronous Operation With Full Initial Load.....	80

Figure 5.20 PCC Voltage, Asynchronous Operation With Light Initial Load .....	81
Figure 5.21 Real and Reactive Power Transfer, Asynchronous Operation With Light Initial Load .....	82

## 1 Introduction

This study analyzes the performance of two D-STATCOMs operating in parallel on a power grid. It compares the performance of two D-STATCOMs operating on the same PCC versus a single D-STATCOM. It also analyzes the effect that a parallel full-wave rectifier has on the performance and stability of a D-STATCOM. PSCAD software is used to model and simulate these devices and their interaction with the grid and with a load.

### 1.1 Sustainability

Over the past decade, sustainability has risen from an overlooked ideal to a mainstream concern. A significant amount of research and money has been dedicated to improving the sustainability of resource-intensive processes as well as utilizing renewable forms of energy. Great advances have been made in improving the efficiency of energy-hungry appliances. The increased importance of sustainability combined with the ever-increasing cost of gasoline has contributed to the average adjusted fuel economy of automobiles in the United States increasing by 22% between 2004 and 2012 [1].

Renewable energy resources have also exploded in popularity, especially in the past few years. Figure 1.1 shows the worldwide growth of all renewable energies and Figure 1.2 shows the growth of solar installations in the United States. Solar photovoltaic installations have become increasingly popular as its cost per kilowatt plummets and incentives for installation are offered. In fact, worldwide solar generation grew by a factor of 49 between 2000 and 2012 [2]. Technological advances have also improved the efficiencies of solar cells, allowing more power to be generated in a smaller footprint.

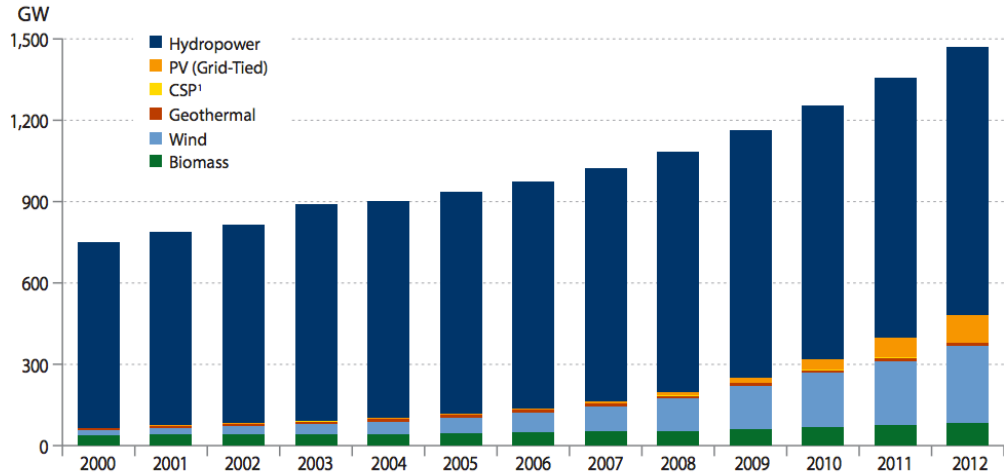


Figure 1.1 Global Renewable Energy Capacity [2]

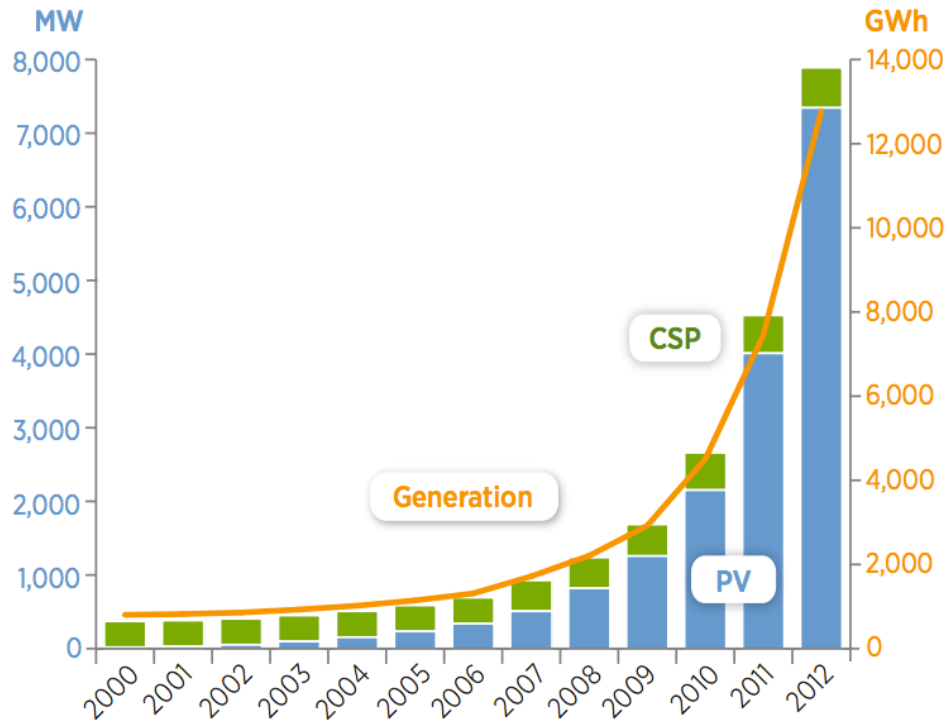


Figure 1.2 U.S. Installed Solar Capacity and Yearly Generation [2]

## 1.2 Increased Electrical Energy Consumption

Even with the actions we have taken to promote sustainability, worldwide electrical energy consumption continues to rise. As the world population increases, the demand for energy continues to increase. In addition to previously un-electrified parts of the world gaining access to electrical energy, other regions of the world continue to increase their per-capita demand for electricity. Figure 1.3 shows how large countries such as China have drastically increased their per capita energy consumption since the turn of the century. Worldwide, total electrical energy consumption has increased by around 40% since 2000 [3]. Even as more efficient appliances are installed in the homes of consumers across the world, demand continues to rise due to the increasing number of devices that consume electrical energy, such as electric cars and a myriad of consumer electronic devices.

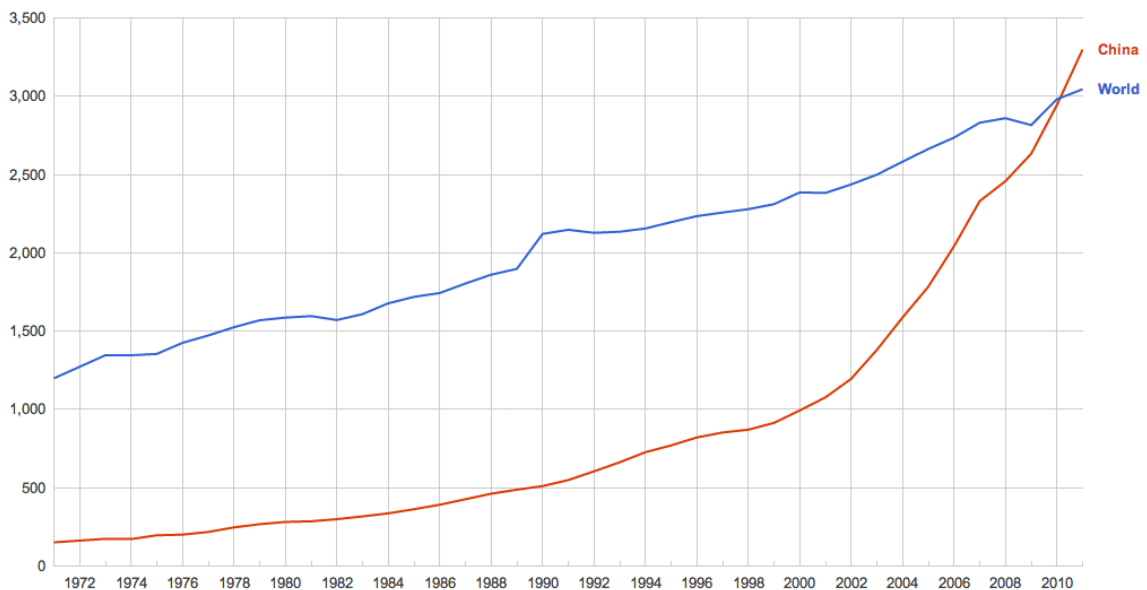


Figure 1.3 Per Capita Energy Consumption in China and Worldwide [4]



### 1.3 Impact on Power Quality

The ever-increasing demands placed on the grid combined with the inherent challenges of renewable energy have negatively impacted power quality. Many of today's loads are highly nonlinear, resulting in non-sinusoidal voltage waveforms with unwanted harmonics. This in turn can interfere with the normal operation of sensitive equipment. Additionally, surges and swells caused by faults, among other things, cause changes in the grid voltage that can be harmful to the equipment of end users and can cause instability in the grid. The Northeast Blackout of 2003 is a glaring example of how a single fault can contribute to significant voltage sags, power surges, instability, and ultimately widespread power outages [5].

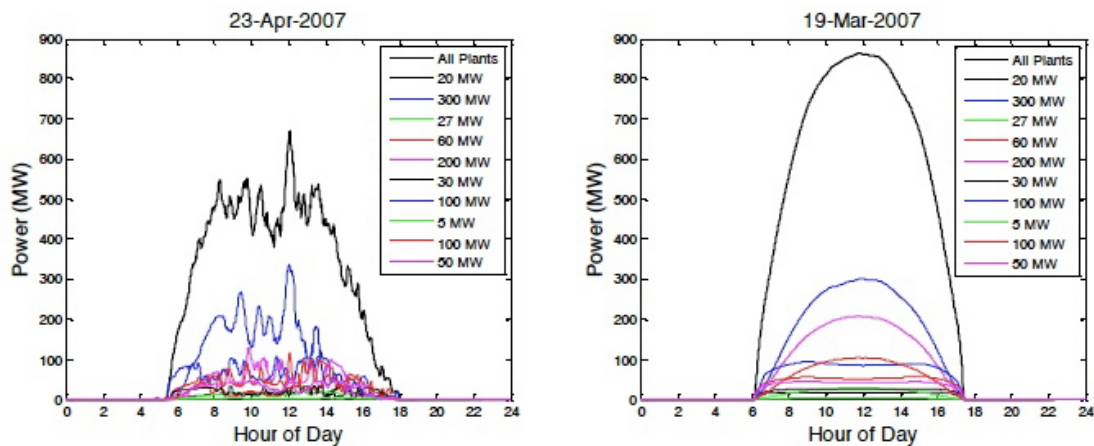


Figure 1.4 Large Scale PV Output on Cloudy (Left) and Clear (Right) Days [6]

Renewable energy installations, particularly photovoltaic systems, have also presented a challenge to grid operators. Because of their highly intermittent nature, PV can negatively affect the stability and power quality of the grid. One cloud can quickly and significantly decrease the power production of a solar system, resulting in grid voltage fluctuations. In large PV installations, these swings can be significant. As seen in

Figure 1.4, PV power output is shown in several large installations in the Nevada area. On a cloudy day, the power swing can be over 200 MW in a matter of minutes.

Conventional grid technology has only limited ability to compensate for such rapid fluctuations in power. Spinning reserves can be used to compensate for fluctuations of power, but these reserves are intended to compensate for another generation facility going offline, not to react to quick power fluctuations due to the intermittency of renewable energy. Using spinning reserves to compensate for the intermittencies of solar PV, for example, is both costly and inefficient. However, thanks to advances in power electronics, new devices are capable of quickly reacting to sags and swells in the grid.

#### **1.4 FACTS Controllers**

Advances in power electronics have paved the way for revolutionary changes in how many systems are capable of operating. From consumer electronics to HVDC, power electronic devices have improved efficiencies of systems and decreased sizes of devices. Power electronic devices have also paved the way for flexible AC transmission system (FACTS) equipment that is capable of continuously controlling the flow of power in a grid as well as improving the power quality for customers.

FACTS can improve grid stability by quickly and continuously injecting voltage or current into a transmission line. If a quick change in power flow is detected, FACTS controllers are able to quickly react to ensure that transmission lines remain optimally loaded. This makes FACTS controllers ideal for managing the intermittent power coming from renewable resources such as solar and wind. Furthermore, by precisely controlling the power flowing through a transmission line, FACTS controllers can safely push

transmission lines closer to their thermal limit, thus reducing the need to build new lines to satisfy demand.

This study focuses on the STATCOM, a FACTS controller that operates as a voltage source converter to deliver or sink variable reactive power to a transmission line. STATCOMs use fully controllable switches such as Insulated Gate Bipolar Transistors (IGBT) or Gate Turn-Off Thyristors (GTO), which result in less harmonic content than similar devices such as static var compensators. STATCOMS generally use a capacitor as the dc source. This capacitor is fed from antiparallel diodes connected across each of the six switches. Because of the relatively limited energy storage of a capacitor, STATCOMs are only effective at controlling reactive power. However, if an energy source such as a battery bank or a solar system feeds the dc source, STATCOMs can also deliver real power similarly to a grid tie inverter. The typical application of a STATCOM is shown in Figure 1.5.

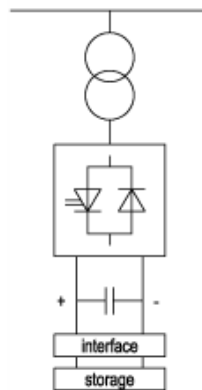


Figure 1.5 Typical STATCOM Application [7]

## 2 Background

### 2.1 Power Flow in Transmission Lines

Power flow through any portion of the grid, including both the transmission level and the distribution level, is subject to circuit laws. Since the impedance of a line is mostly inductive, the inductance of a line is the primary determinant of power flow through a grid for a given load. As can be seen in the equations below, both real and reactive power flow between two busses is a function of the voltages at both busses, the impedance of the line, and the phase angle between the two busses [8].

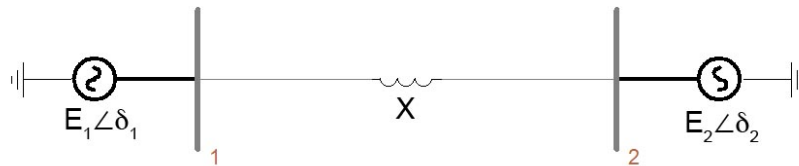


Figure 2.1 Two-Bus System

$$\text{Real power flow: } P = \frac{E_1 E_2}{X} \sin \delta \quad (2.1)$$

$$\text{Reactive power flow at Bus 1: } Q = \frac{E_2(E_2 - E_1 \cos \delta)}{X} \quad (2.2)$$

$$\text{Where } \delta = \delta_1 - \delta_2 \quad (2.3)$$

Nearly every grid operates in a much more complex manner; however, system operators need to be able to control power flow through a grid based on factors such as

power supply and demand, contracts with line owners, and thermal limits. Also, customers expect their voltage to remain constant [8]. As a result, system operators manipulate three of the four parameters to control the flow of power: the source voltage, the line impedance, and the phase angle between the two busses. Before the advent of FACTS controllers, less sophisticated methods of manipulating these parameters were utilized exclusively.

One simple method to increase power flow in a transmission line is by simply adding capacitors in series with the line, as shown in Figure 2.2. The series capacitance is a negative reactance that serves to lower the overall reactance of the transmission line. This in turn lowers the impedance of the line, resulting in an increase in both real and reactive power transfer. By lowering the impedance of the line, series capacitors also reduce flicker during brief periods of heavy loading, such as when a motor is starting up [9]. The main disadvantage of this approach is that the impedance of the transmission line cannot be adjusted. Series capacitor banks also require protection to prevent high currents from flowing through them during faults [10].

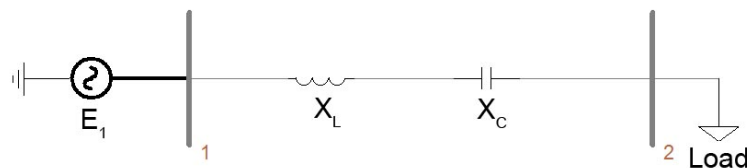


Figure 2.2 Series Capacitor in Two-Bus System

Another device for improving the controllability of power flow is the shunt capacitor bank. They are typically used to support voltage near a load with a low and lagging power factor. Shunt capacitor banks can either be fixed or switched. Their

switching frequency is generally on the order of twice a day: once to switch on during the time when heavy loads come online and once at night when the load is light [10]. Switched shunt capacitors improve the controllability of power flow by improving the voltage regulation at the load. This also improves the power quality to the customer. Figure 2.3 shows a typical implementation of a switched shunt capacitor bank.

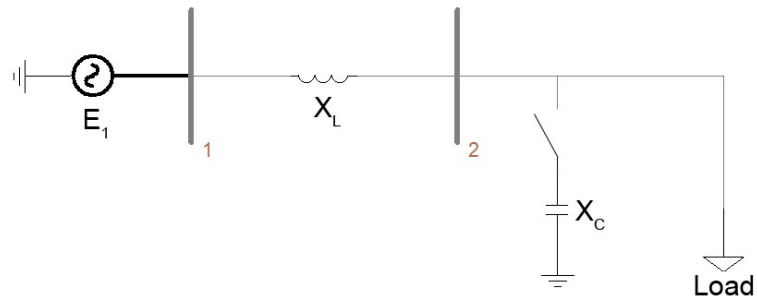


Figure 2.3 Switched Shunt Capacitor

Voltage control at the source can be achieved using a load tap-changing transformer. These transformers have secondary windings with several automatically or manually selectable taps. By changing the tap, the turns ratio of the transformer also changes, thus adjusting the secondary voltage of the transformer. Under periods of high load, the taps are changed so that the secondary output voltage increases enough to maintain a relatively constant voltage at the load. These transformers usually have 32 steps to provide output voltages in the range of nominal voltage  $\pm 10\%$  [11].

Phase-shifting transformers can control the flow of power by controlling the phase angle between two busses on the grid. There are several ways to implement a phase-shifting transformer. In the asymmetric configuration, a delta-connected transformer with a tap-changing secondary is connected in shunt with the transmission

line. Transformers are then connected in series with each phase of the transformer, with their secondary windings connected in a Y configuration. The secondary windings of the delta transformer are then connected to the secondary windings of the series transformers. The line-to-line angles of the delta transformer secondary windings are 90 degrees out of phase with the phase angles of the source. The phase-shifted secondary voltage is then effectively added to the source via the series transformers. Thus, by controlling the magnitude of the phase-shifted voltage via tap-changing, the phase angle of the output voltage can be controlled. Phase-shifting transformers are typically used when power flow control is needed across different paths in meshed networks [12].

While all of these devices improve the controllability of power flow and the power quality to the customer, there are a few disadvantages. Firstly, adjustable devices such as tap changing transformers and switched shunt capacitors are typically unable to quickly and frequently change because of their mechanical means of control. Also, continuously adjustable power flow control is not possible with any of these devices. FACTS devices eliminate both of these problems by using power electronics to control power flow [8].

## **2.2 Power Flow and FACTS Devices**

FACTS devices use semiconductor switches and other conventional components to quickly and continuously adjust the flow of power. This results in several important advantages over conventional power control equipment. Since conventional power control equipment can only compensate for steady-state loading, transmission lines using this equipment must be conservatively rated to prevent overloading during transient conditions. FACTS controllers can compensate for transient loads, which results in an

increase in power transmission capability as well as improved power quality and stability [13]. FACTS devices can be categorized into three main segments: series controllers, shunt controllers, and dynamic energy storage devices [14]. Additional topologies such as combined series-series controllers and combined series-shunt controllers [8] will not be discussed in this study.

### 2.2.1 Series Controllers

Series controllers work by injecting voltage into the line with which they are series-connected. This effectively changes the impedance of the overall line [15]. One common type of series FACTS device is the Thyristor-Controlled Series Capacitor (TCSC). The TCSC consists of a thyristor-controlled reactor in parallel with a capacitor bank, as seen in Figure 2.4. Often times, there are additional mechanically switched capacitor banks in series with the TCSC to provide additional negative reactance to the line [14].

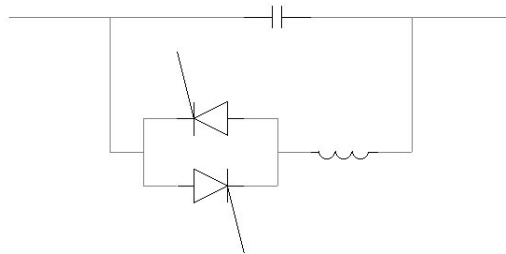


Figure 2.4 Thyristor-Controlled Series Capacitor

The firing angles of the thyristors are used to control the current flowing through the inductor and thus the overall reactance of the device. As seen in Figure 2.5, increasing the firing angle from 0 degrees to a critical level increases the inductance of the device. After this firing angle, there is a critical region where parallel resonance occurs. In this



region, the reactance of the TCSC approaches infinity [8]. The TCSC acts as a capacitor from the upper limit of the resonance region to 180 degrees [16].

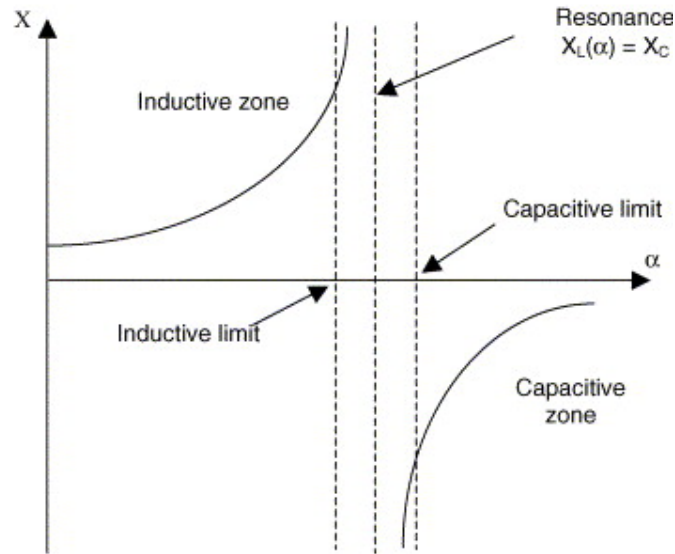


Figure 2.5 Reactance vs. Firing Angle for TCSC [16]

## 2.2.2 Shunt Controllers

Shunt controllers work by injecting current into the bus with which they are connected [15]. As a result, they regulate the voltage at the bus. This improves grid stability and power quality [14]. It also increases the power transfer capability of a line by decreasing the voltage across the line. There are a variety of shunt controllers, some of which are discussed below.

### 2.2.2.1 Static Var Compensator

The Static Var Compensator (SVC) is a type of shunt compensation that has several possible configurations. In general, the SVC consists of a capacitor or reactor that is controlled by thyristors and connected in shunt to a bus, as well as a harmonic filter. The result is a device that can quickly deliver continuously controllable reactive power

[14]. Figure 2.6 shows several components of an SVC, as well as how they are interconnected to the grid.

One component of the SVC is the Thyristor-Controlled Reactor (TCR). This consists of a reactor connected in series with two antiparallel thyristors, which is then connected in shunt to a bus. The firing angles of the thyristors can be continuously controlled to consume a continuously controllable amount of reactive power [17].

Thyristor-Switched Capacitors (TSC) are also used in SVCs to supply reactive power. TSCs consist of a capacitor connected in series with two antiparallel thyristor, which is then connected in shunt to the bus. Unlike TCRs, the thyristors of TSCs operate in full conduction or zero conduction. Thus, TSCs are not continuously controllable [18].

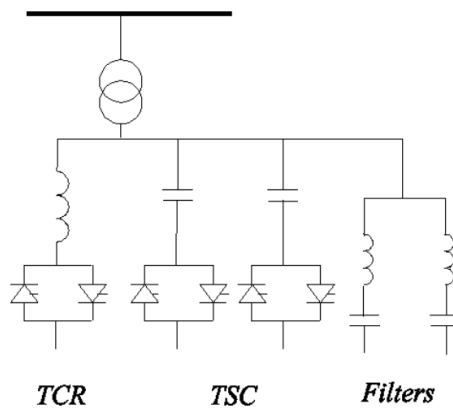


Figure 2.6 Components of a Static Var Compensator [14]

### 2.2.2.2 STATCOMs

The Static Synchronous Compensators (STATCOM) is another type of shunt controller. However, unlike first-generation FACTS controllers, which use semi-controllable switching devices (thyristors), STATCOMs are considered a second-generation controller. Second-generation controllers use fully controllable switches such

as Gate-Commutated Thyristors (GCT), GTOs, or IGBTs. By using fully controllable switches, switches can be controlled with Pulse Width Modulation (PWM). The PWM carrier frequency can be much higher than the line frequency, resulting in less filtering requirements and improved harmonic performance [8]. IGBTs and GCTs also require simpler gate drives than the thyristors used in SVCs. These advantages also serve to reduce the overall installation size of a STATCOM: A typical STATCOM occupies about 50% of the space required for a similarly-sized SVC [7].

In addition to better harmonic performance, STATCOMs have another important advantage over other shunt controllers such as SVCs. Unlike SVCs, STATCOMS can supply constant current over a wide range of voltages. SVC current is limited by the voltage of the Point of Common Connection (PCC) and the reactances of the passive components [9]. This characteristic is shown in Figure 2.7.

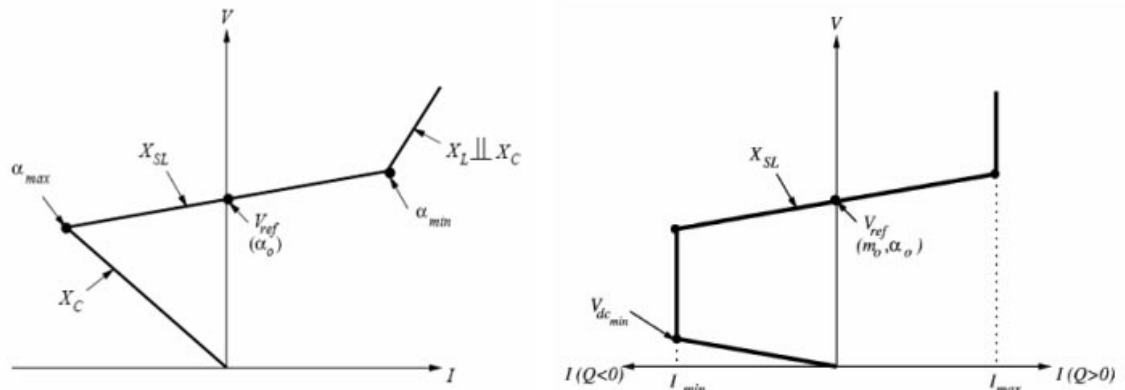


Figure 2.7 I-V Characteristics for SVC (Left) and STATCOM (Right) [17]

STATCOMs are a voltage source converter (VSC) that can source or sink reactive power to the PCC. By sourcing or sinking reactive power, a STATCOM acts as a voltage

regulator for the PCC to which it is connected [19]. As seen in Figure 2.8, a typical STATCOM has a similar topology to a three-phase inverter with a capacitor supplying the dc voltage.

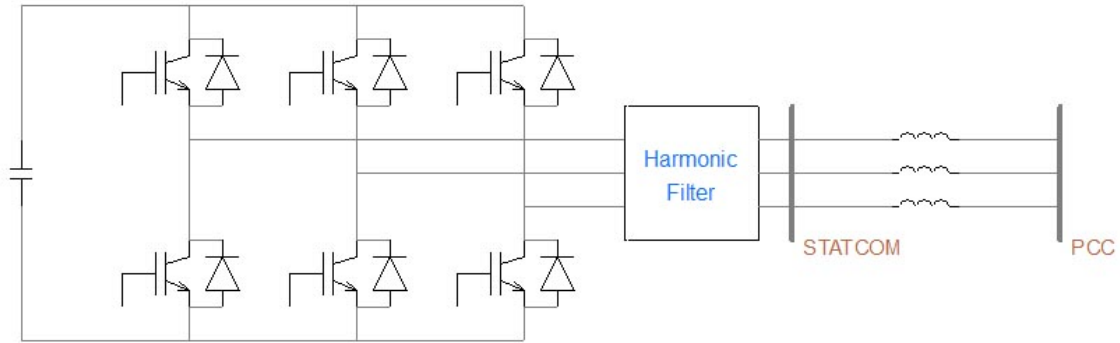


Figure 2.8 Simplified STATCOM Schematic

The dc capacitor charges from the energy stored in the reactance from the transformer. This energy is discharged through the antiparallel diodes across the IGBTs into the dc capacitor, similarly to the operation of a boost converter. The IGBTs are triggered using Sinusoidal Pulse Width Modulation (SPWM) to produce a three-phase waveform that is then filtered, resulting in a three-phase sinusoidal output. Since a grid-fed capacitor is generally the only dc source for a STATCOM, no active power can be supplied by a STATCOM. However, a continuously adjustable amount of reactive power can be sourced or sunk by controlling the magnitude of the STATCOM bus voltage. Active power is kept as close to zero as possible by keeping the phase angle between the STATCOM bus and the PCC bus as close to zero as possible. The reactance between these two busses is generally provided by the leakage reactance of the transformer connecting the busses [19].

### 2.3 Thesis Objective

The goal of this thesis is to study and analyze the performance of two small STATCOM devices operating in parallel, as shown in Figure 2.9. The two STATCOMs are rated at 1 Mvar each and interconnect with the PCC at 12 kV through two 480V/12kV transformers. This system is a type of Distribution STATCOM (D-STATCOM). D-STATCOMs are intended to be placed at points in a distribution system where improved voltage regulation is required. They tend to be smaller in both size and capacity than a STATCOM intended for use in a transmission system.

This D-STATCOM is unique because it employs a three-phase full-wave rectifier that links the ac side of the D-STATCOM to the dc side. The rectifier is intended to provide a continuous connection between the two sides, which may result in faster charging of the dc capacitor.

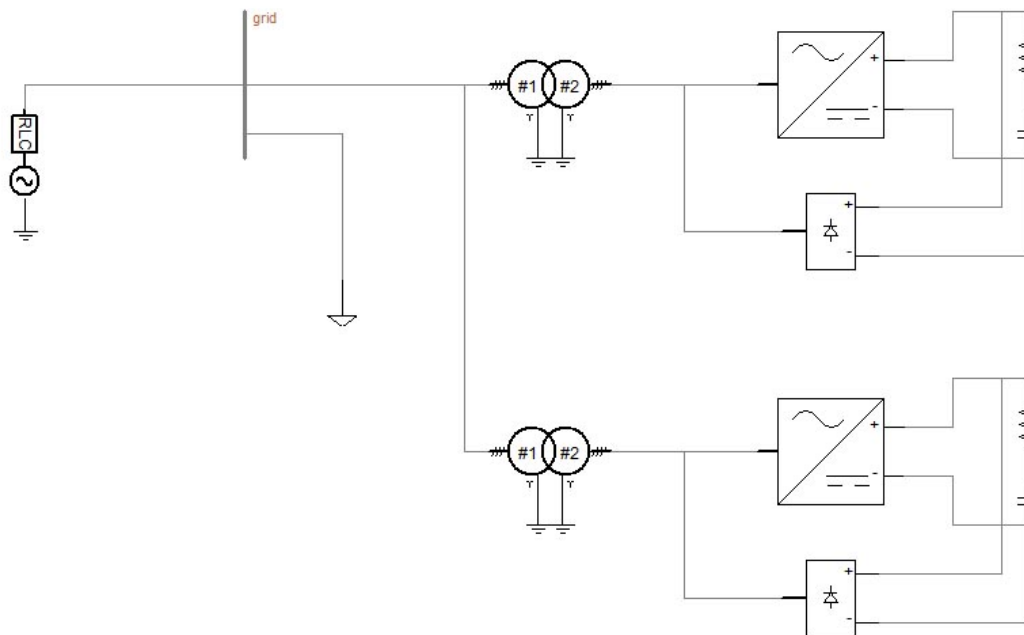


Figure 2.9 Parallel STATCOM System Overview

There is a variety of literature on the modeling and simulation of both STATCOMs and D-STATCOMs [19][20][21], but these studies focus on the voltage regulation performance of a single STATCOM. There is little information available on the operation of two or more STATCOMs connected in parallel to the same PCC. Furthermore, no literature mentions the inclusion of the parallel three-phase rectifiers that bypass the VSC, as shown in Figure 2.9. Thus, the benefits and/or drawbacks of such a configuration are unknown.

This study will model and analyze the performance of the system using PSCAD software. The study will examine the performance of the system when both STATCOMs are operated independently and when they are operated synchronously. Transient and steady state response of the system will be considered, as well as Total Harmonic Distortion (THD) performance and operation under different load conditions. Lastly, the significance of the parallel rectifiers shown in Figure 2.9 will be examined in order to determine their effect on several characteristics of operation of the D-STATCOM, including initial charge time for the dc capacitor, power loss of the system, and stability of the system.

### 3 Design Requirements

The parallel D-STATCOM model is based on previous research done in [22] using RSCAD to simulate the system. RSCAD is a software suite by RTDS Technologies that allows engineers to model and simulate power systems using physical hardware. This allows for real-time simulation of complex power systems using actual hardware. Complete RTDS systems are capable of solving a system consisting of hundreds of nodes with 50 microsecond time steps in real time [23]. An assortment of RTDS hardware racks can be seen in Figure 3.1.



Figure 3.1 RTDS System Racks [24]

Cal Poly does not have access to an RSCAD/RTDS system, but the university does have PSCAD software available. PSCAD is a software suite used for the design and

simulation of power systems in software. It has similar functionality to RSCAD/RTDS, but is entirely software-based and has limited real-time simulation capability. PSCAD provides ample power to simulate the parallel D-STATCOM system.

To develop a reasonable model for parallel D-STATCOM operation, several design requirements must be considered. Firstly, the system model must represent a simple yet practical test case for the D-STATCOMs. Secondly, the D-STATCOMs and their associated equipment must accurately represent their real-world counterparts.

### **3.1 Hardware Requirements**

Each D-STATCOM module is rated for 1 Mvar maximum output. All components of the D-STATCOM must be able to fulfill this requirement. Specifically, the switches and diodes used for the inverter must be capable of passing an adequate amount of current. The dc capacitor must also be sized to store enough energy to produce this level of reactive power without excessive voltage ripple. The switches used for the inverter must be fully controllable. Each transformer connecting the D-STATCOM to the PCC must be rated for 1 MVA. The line-to-line voltage of the D-STATCOM is 480 V. The PCC voltage is 12 kV. As per IEEE 519, THD for the ac connection of the D-STATCOM should be below 5% [25]. Both the output filter and the SPWM generator must be designed to meet this standard.

### **3.2 Control Requirements**

The control system for each D-STATCOM must be able to maintain both a stable ac voltage and a stable dc voltage during normal operation and during its initial turn-on period. The control system must also remain stable when two D-STATCOMs are



operating on the same PCC. The control system must also prevent the reactive power output of the D-STATCOM from exceeding 1.0 Mvar.

### **3.3 System Requirements**

The PCC must be fed by two transformer-connected D-STATCOMs, as well as by a grid supply. One or more complex loads must also be connected to the PCC to simulate various levels of loading on the PCC. Circuit breakers are necessary on all connections to facilitate power flow control to all components of the system.

## 4 PSCAD Model and Simulation

### 4.1 System Components

The PSCAD model of the parallel D-STATCOM system consists of several basic components as well as several modules. The top-level PSCAD schematic can be seen in Figure 4.1.

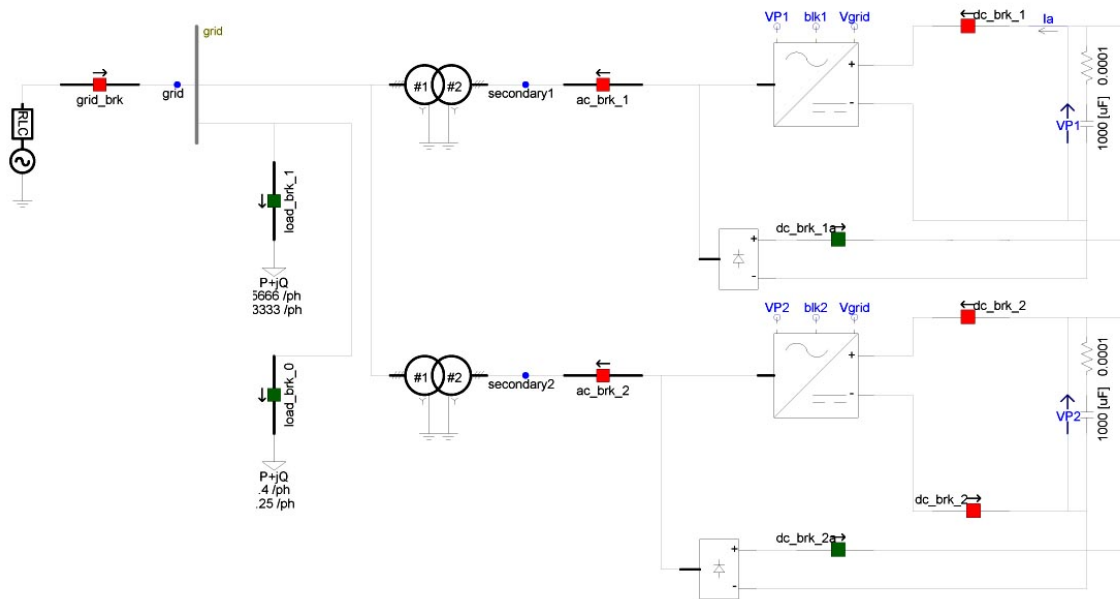


Figure 4.1 PSCAD Parallel D-STATCOM System Top Level Schematic

As seen above, the system consists of an ac grid voltage source connected to the PCC by a finite impedance. Complex loads are also connected to the PCC, as well as two transformers. Each of these two transformers connects the ac side of their respective D-STATCOM module to the PCC. The dc side of each D-STATCOM is connected to a capacitor with a series resistance. Three-phase full-wave rectifiers also connect the ac side of each D-STATCOM to its dc side. Lastly, circuit breakers are used to isolate each module of the system.

### 4.1.1 Grid Voltage and Impedance

The voltage source for the grid is 12 kV, line-to-line. The frequency is 60 Hz. These values correspond to typical distribution voltage and frequency values in the United States [26].

The original line impedance used in [22] is  $5.675 + j7.832 \Omega$ . This value is also used in the PSCAD model. The three-phase resistance is thus  $5.675 \Omega$  and the three-phase inductance is 20.775 mH. The inductance is a function of frequency and reactance, as shown in ( 4.1 ) and ( 4.2 ).

$$L = \frac{X}{\omega} \quad (4.1)$$

$$\omega = 2\pi f \quad (4.2)$$

The three-phase voltage source with series R-L-C impedance is used to implement the voltage source in PSCAD. The above resistance and inductance are used as the respective parameters in the PSCAD voltage source. The capacitance parameter is set to zero.

### 4.1.2 Load

The load for the system is connected to the PCC, similarly to the typical configuration for a D-STATCOM installation. The original model used in [22] implements a load that draws 1.7 MW and 1.0 Mvar.

The load for this study consists of two separate components. The first component is a load that draws 1.7 MW and 1.0 Mvar. The second component is a 1.2 MW and 0.75 Mvar load. Activating these two loads at the same time or independently of one another

allows for the modeling of several possible load profiles that facilitate the testing of step response, low load conditions, and high load conditions.

The two components of the load are implemented in PSCAD using the three-phase fixed load component. The power parameters for this component are measured per-phase, so the rated real and reactive power per phase is equal to one-third of the values stated on the previous page. Likewise, the rated voltage parameter for this component is measured line-to-ground, so the value for this parameter is  $\frac{12 \text{ kV}}{\sqrt{3}} = 6.928 \text{ kV}$ . The three-phase fixed load component automatically adjusts the resistance and reactance of the load to maintain a constant power draw independent of the bus voltage. Circuit breakers with timed breaker logic are used to connect and disconnect the load components from the PCC.

### **4.1.3 Transformers**

Each D-STATCOM module is connected to the PCC through a three-phase transformer. As in [22], a 12 kV/480 V Y-Y transformer with the neutral points grounded. Just like each D-STATCOM, each transformer is rated for 1 MVA. The ideal transformer model is used and a leakage reactance of 0.1 per unit is used. This value is chosen because it is representative of a typical leakage reactance of a medium-sized transformer [28].

In addition to transforming the voltage levels between the D-STATCOMs and the PCC, the transformers also serve an important role in controlling power flow. The leakage reactance of the transformers are used as the reactance component shown in the power flow equations ( 2.1 ) and ( 2.2 ).

In this model, the 12 kV side of the transformers are directly connected to the PCC while the 480 V sides are connected to the D-STATCOMs through circuit breakers controlled by timed breaker logic.

#### 4.1.4 Capacitors

Capacitors are typically used as the only energy storage device in both STATCOM and D-STATCOM systems. This model uses a 36,000  $\mu\text{F}$  capacitor with a 0.1  $\text{m}\Omega$  series resistance, as is the case in [22]. Each capacitor is connected to the dc side of the D-STATCOM with a dc circuit breaker on the positive end of the capacitor-resistor component.

#### 4.1.5 Three-Phase Full-Wave Rectifier

A three-phase full-wave rectifier, as shown in Figure 4.2, connects the ac sides of the D-STATCOMs to their respective dc sides. The resistance values for the diodes are kept at the default PSCAD values of  $R_{\text{on}} = 0.01\Omega$  and  $R_{\text{off}} = 1\text{M}\Omega$ . There is no forward voltage drop across the diodes.

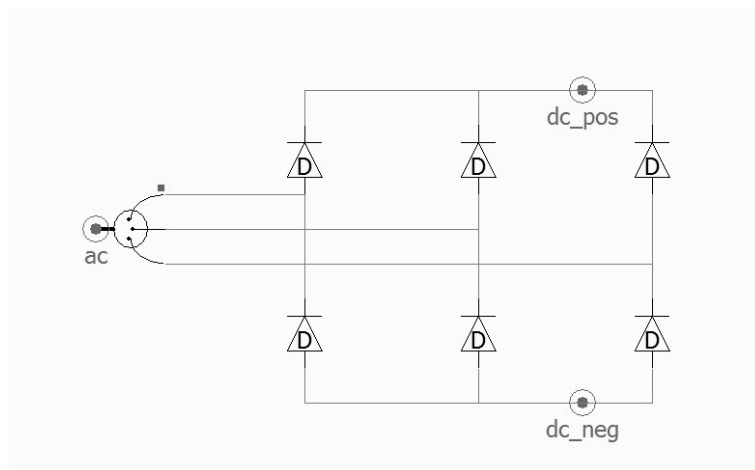


Figure 4.2 Three-Phase Full-Wave Rectifier

The purpose of the full-wave rectifier is unknown and will be investigated in this thesis, as the previous study [22] suggested that it may negatively impact the performance of the system. This effect on performance will also be examined in this study.

## 4.2 The D-STATCOM Module

The D-STATCOM is implemented in PSCAD as a module with several components and one additional sub-module. The D-STATCOM module can be seen in Figure 4.3.

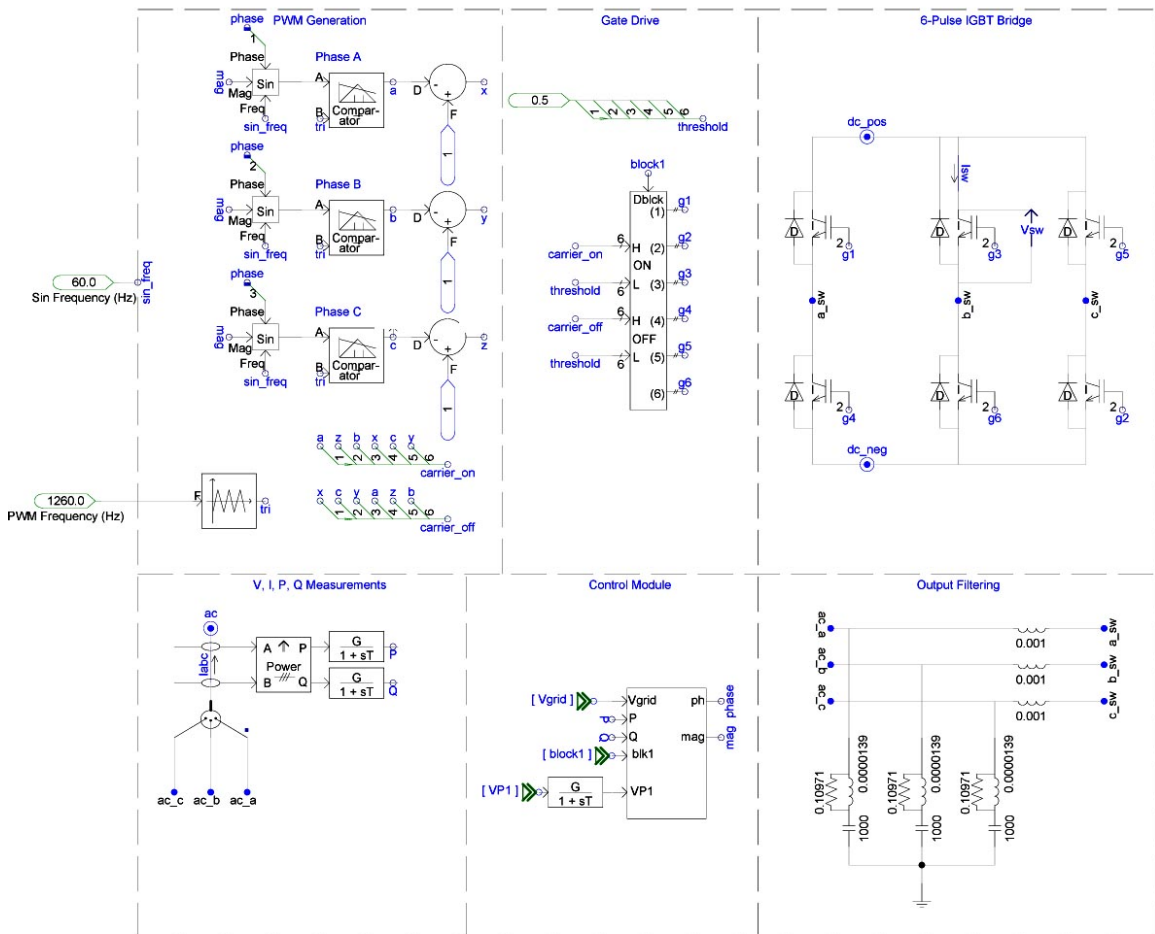


Figure 4.3 D-STATCOM Module

The D-STATCOM module consists of a 3-phase SPWM generator, a six-pulse IGBT gate drive, a six-pulse IGBT bridge, output filtering components, and a control module. Internal measurements of active and reactive power are also included. PSCAD has a variety of Continuous System Model Functions (CSMF) that can be used to generate and manipulate continuous analog signals. CSMF components are used extensively in the D-STATCOM module as well as the control module in order to generate signals and to perform mathematical operations on signals.

#### 4.2.1 SPWM Generator

The SPWM generator works by comparing three sine waves, each with a phase difference of  $120^\circ$  from each other, to a triangle wave. Six signals are generated: one for each phase when the sine wave value is greater than the triangle wave value, and one for each wave when the sine wave value is less than the triangle wave value. A detailed view of the SPWM generator can be seen in Figure 4.4.

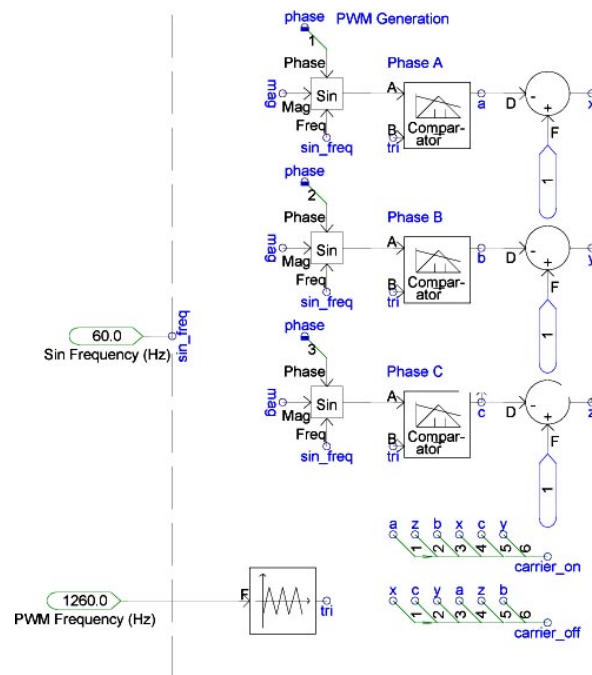


Figure 4.4 SPWM Generator

Three sine waves are generated by the sin function. This function outputs a sine wave based on three inputs: phase, magnitude, and frequency. The frequency is set to 60 Hz for all three phases. The phase and magnitude values are generated by the control module. The magnitude of the sine wave generators can be controlled between values of zero and one.

The triangle wave generator creates a triangle wave with a 50% duty cycle and an amplitude of 1. The frequency selected for the triangle wave is 1260 Hz because this is a triplen harmonic of 60 Hz, resulting in improved harmonic performance [8]. 1260 Hz is also a high enough frequency that filtering requirements are reasonable, while still being low enough that switching losses are also reasonable.

The modulation index of a PWM scheme is the ratio between the reference signal amplitude and the carrier signal amplitude. In the case of the D-STATCOM model, the triangle wave has a fixed magnitude of one, so the modulation index is equal to the magnitude of the sine waves. Since the sine waves can have magnitudes between zero and one, the modulation index can subsequently take on values between zero and one. By limiting the modulation index to between zero and one, the filtered SPWM output magnitude has a linear relationship with the modulation index. Figure 4.5 shows the relationship between modulation index and the filtered SPWM output magnitude. Keeping the modulation index below one also reduces harmonic distortion by preventing the reference signal from clipping the PWM output.



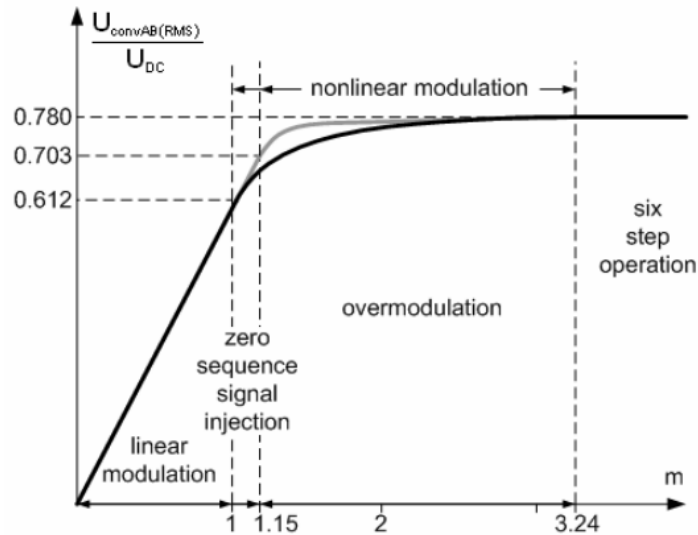


Figure 4.5 RMS Output Magnitude vs. Modulation Index [29]

The three sine waves are fed into three comparators. These three comparators output one when the value of the sine wave is greater than the value of the triangle wave, and zero when the value of the sine wave is less than or equal to the value of the triangle wave. The outputs of the comparator are then inverted by subtracting one from the output values. The three comparator values as well as their inverted values are then sent to the six-pulse IGBT gate drive. When the output of the comparator for any given phase is high, its corresponding high-side IGBT is turned on and its low-side IGBT is turned off. This operation will be described in detail in later sections. Figure 4.6 shows the triangle carrier wave and the sinusoidal reference wave, as well as the non-inverted PWM output waveform, for one phase of the SPWM generator.

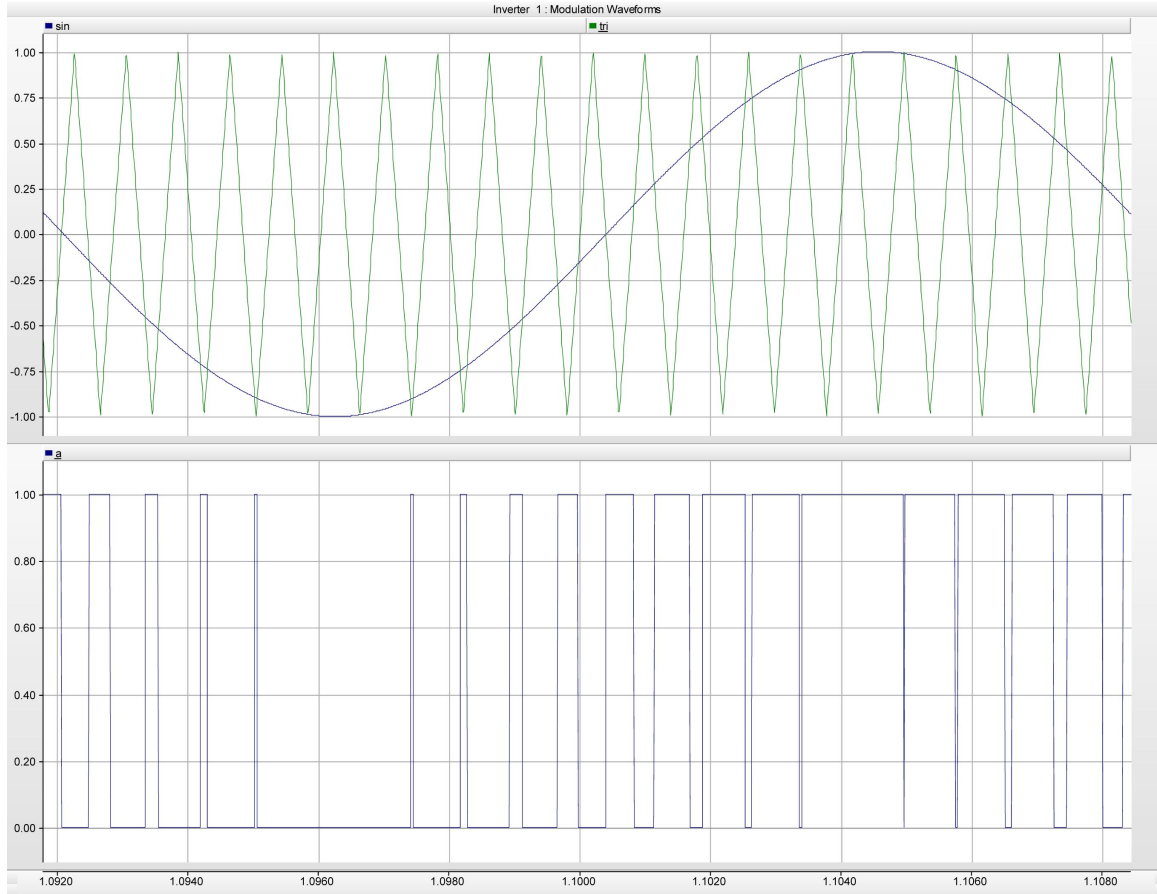


Figure 4.6 SPWM Reference and Carrier Waveforms (top) and PWM Waveform  
(bottom)

#### 4.2.2 Six-Pulse IGBT Gate Drive

PSCAD has a variety of power electronics components that can be used for FACTS and High Voltage DC modeling. One such component is the interpolated firing pulse generator and it is the basis for the six-pulse IGBT gate drive. The interpolated firing pulse generator uses a data array input to generate firing pulses for several kinds of semiconductor switches.

For this study, the interpolated firing pulse generator is configured to generate pulses for GTOs, which have the same triggering characteristics as IGBTs in PSCAD. It is also configured as a six-pulse generator with a block/deblock signal to turn the

generator on and off in tandem with the rest of the D-STATCOM. This configuration can be seen in Figure 4.7.

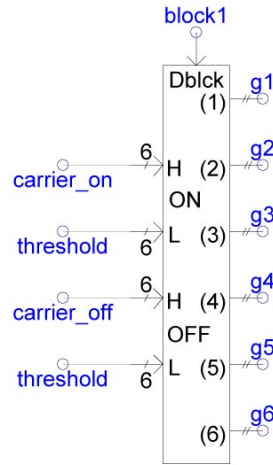


Figure 4.7 Six-Pulse IGBT Gate Drive

The generator turns each IGBT on when its respective element of the ON-H input is greater than its element in the OFF-H input. Likewise, it turns each IGBT off when its respective element of the OFF-H input is greater than its element in the OFF-L input. The *threshold* array consists of six elements, each with a value of 0.5. The *carrier\_on* and *carrier\_off* arrays are generated from the SPWM generator and can be seen at the bottom of Figure 4.4. The *block1* signal is controlled by timed breaker logic at the top level of the system. Each gate output is a two-element interpolated firing array that is fed to its respective IGBT.

### 4.2.3 Six-Pulse IGBT Bridge

The six-pulse IGBT bridge inverts the dc voltage from the capacitor into a high-voltage SPWM waveform by using power electronic switches. Six switches are used to create a three-phase output. The schematic can be seen in Figure 4.8. Three high-side switches and three low-side switches are interconnected as shown in the schematic. Gate

drive signals  $g1$  through  $g6$  control whether the switch is conducting or not conducting. These signals come from the six-pulse IGBT gate drive. Each high-side switch must not be conducting when its corresponding low-side switch is conducting and vice versa, otherwise shoot-through will occur. Shoot-through occurs when both a high-side and the corresponding low-side switch conduct at the same time, effectively shorting the dc supply and causing a large amount of power to be dissipated by the switches. This can reduce the efficiency of the system at best, and cause failure of the switches and/or other components of the system at worst. Shoot-through is inherently prevented when modeling the system in PSCAD, but a real-world implementation of the system must take this into account.

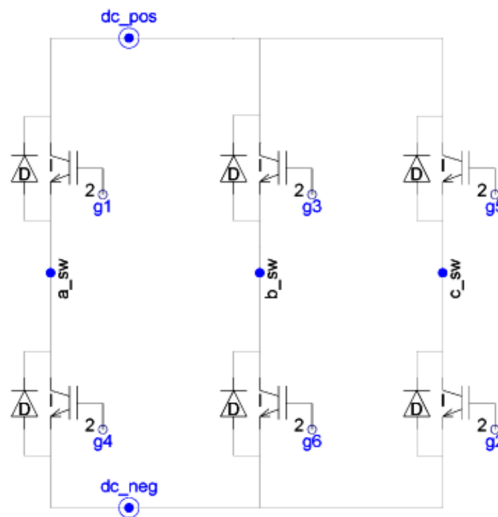


Figure 4.8 Six-Pulse IGBT Bridge Schematic

At the heart of any VSC are switching devices used to invert the dc voltage source into an ac voltage source. For the D-STATCOM model, IGBTs are chosen as the switching devices because they are fully controllable and have high efficiency and current-carrying capability. In PSCAD, there are only two fully controllable power

electronic switches available: the GTO and the IGBT. Both switches operate in essentially the same way in PSCAD, so the IGBT was chosen for this model.

IGBTs combine the easy voltage-controlled gate drive operation of a MOSFET with the low voltage drop of a bipolar junction transistor. They have a large safe operating area and are capable of conducting large amounts of current [30]. These characteristics make them a popular choice for high power switching applications such as the D-STATCOM.

In PSCAD, the IGBT is characterized by the V-I curve shown in Figure 4.9. Reverse recovery time for the IGBT is assumed to be zero. The parameters used for this model are the default values used in PSCAD and are shown in Figure 4.10.

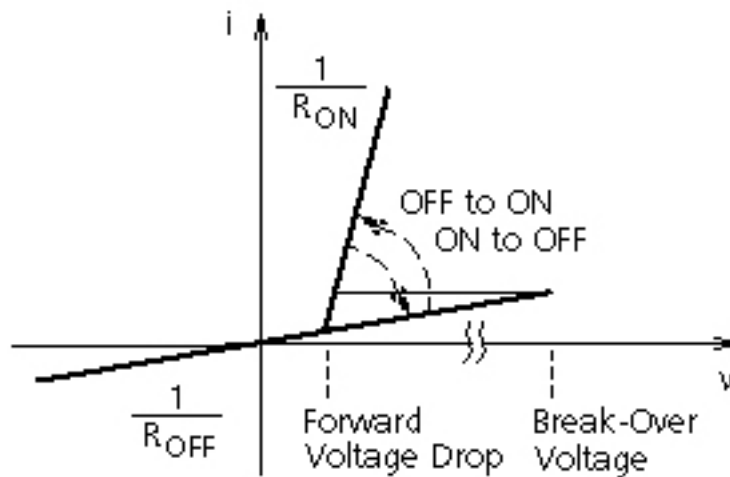


Figure 4.9 V-I Characteristic for IGBT in PSCAD

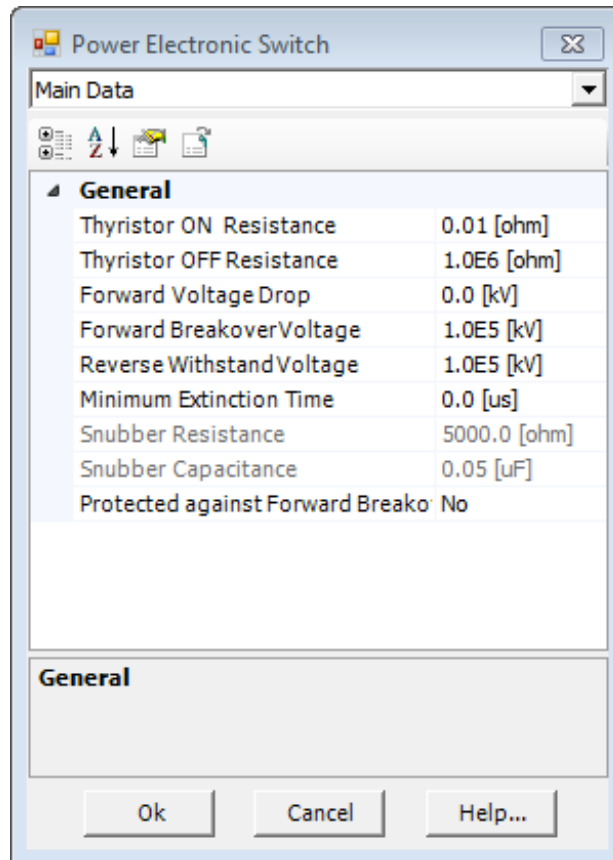


Figure 4.10 Parameters Used for IGBT

Each IGBT has an antiparallel diode connected between the emitter and collector. These diodes allow current to flow from the grid into the dc capacitor and consequently maintain the capacitor voltage. The diodes have a V-I characteristic as shown in Figure 4.11.

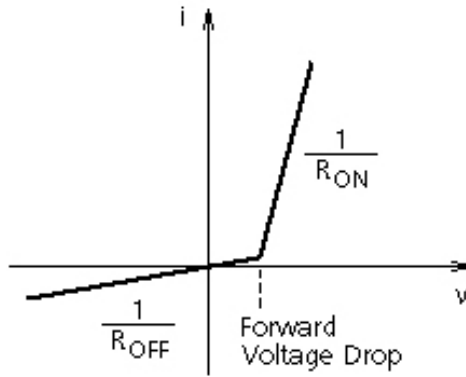


Figure 4.11 V-I Characteristic for Diode in PSCAD

The parameters used for the diode are the default values used in PSCAD and are shown in Figure 4.12.

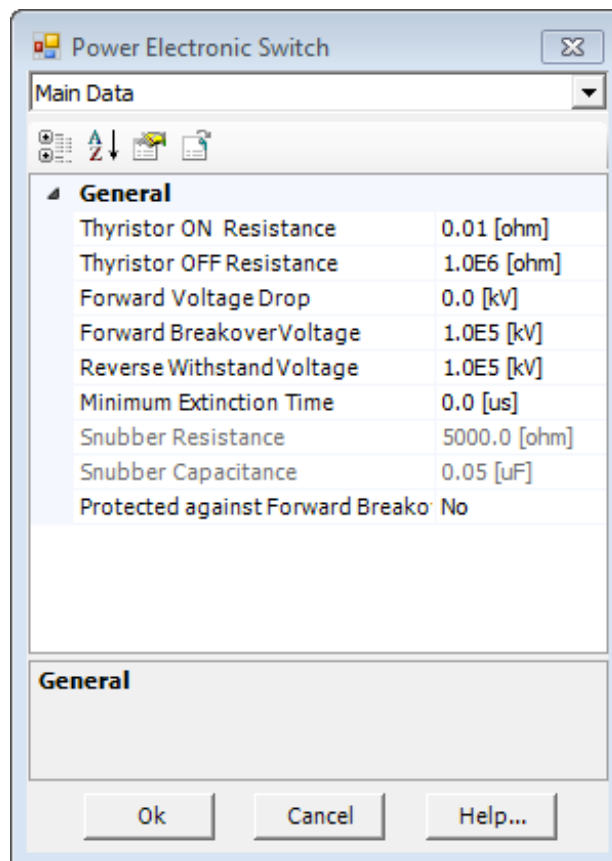


Figure 4.12 Parameters used for Diode

#### 4.2.4 Output Filtering

In order to convert the PWM output signal from the IGBT bridge into a voltage source that can be tied to the grid, output filtering must be used. SPWM creates harmonics above the carrier frequency that must be removed in order to create a sinusoidal output at the frequency of the reference waveform. Since the reference frequency is 60 Hz and the carrier frequency is 1260 Hz, the filter must be able to attenuate at and above the 21<sup>st</sup> harmonic. Thus, an LC low pass filter is used, as shown in Figure 4.13.

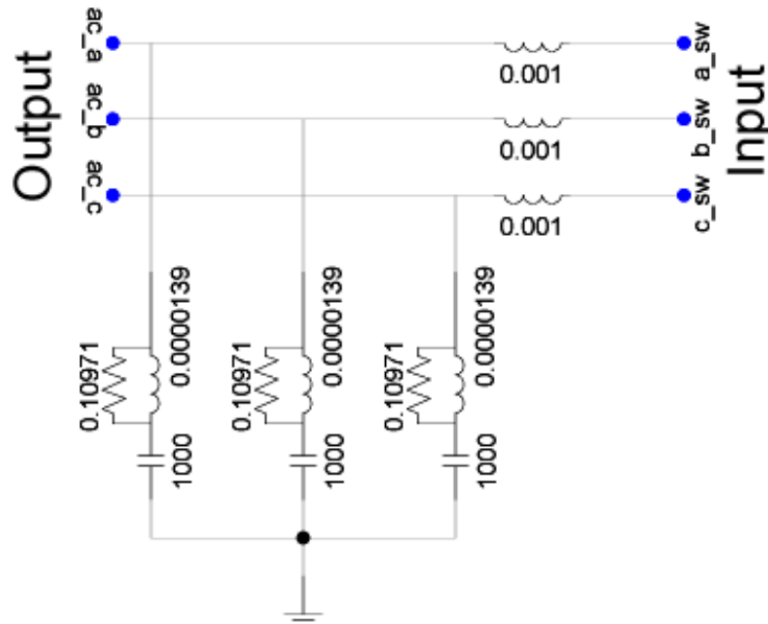


Figure 4.13 Output Filter for D-STATCOM

As can be seen above, the filter consists of inductors in series with the input and output and capacitors in shunt with the output. The capacitors also have equivalent series resistances and equivalent series inductances to improve the accuracy of the model. The capacitors are wye-connected and tied to ground. Inductance values shown above are in Henries, capacitance values are in microfarads, and resistance values are in Ohms. These



values are the same values that are used in [22]. The frequency response of the filter can be seen in Figure 4.14 and the input and output waveforms of the filter can be seen in Figure 4.15. The difference in gain between the reference signal frequency and the carrier signal frequency is 40 dB. The filter becomes resonant at 158 Hz, which is not a harmonic of 60 Hz.

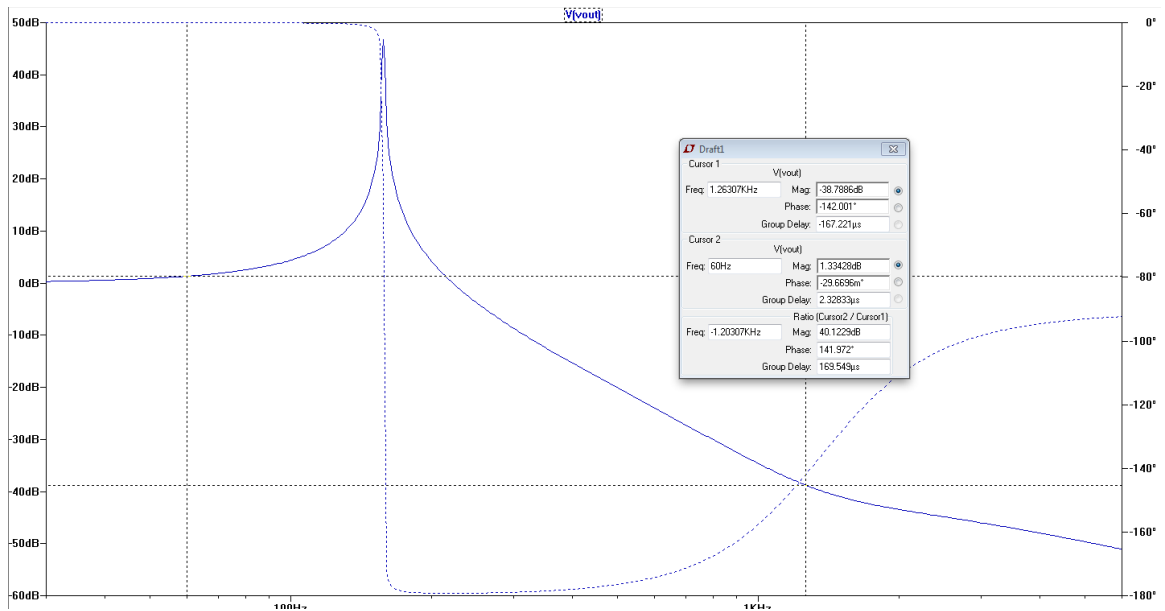


Figure 4.14 Output Filter Frequency Response

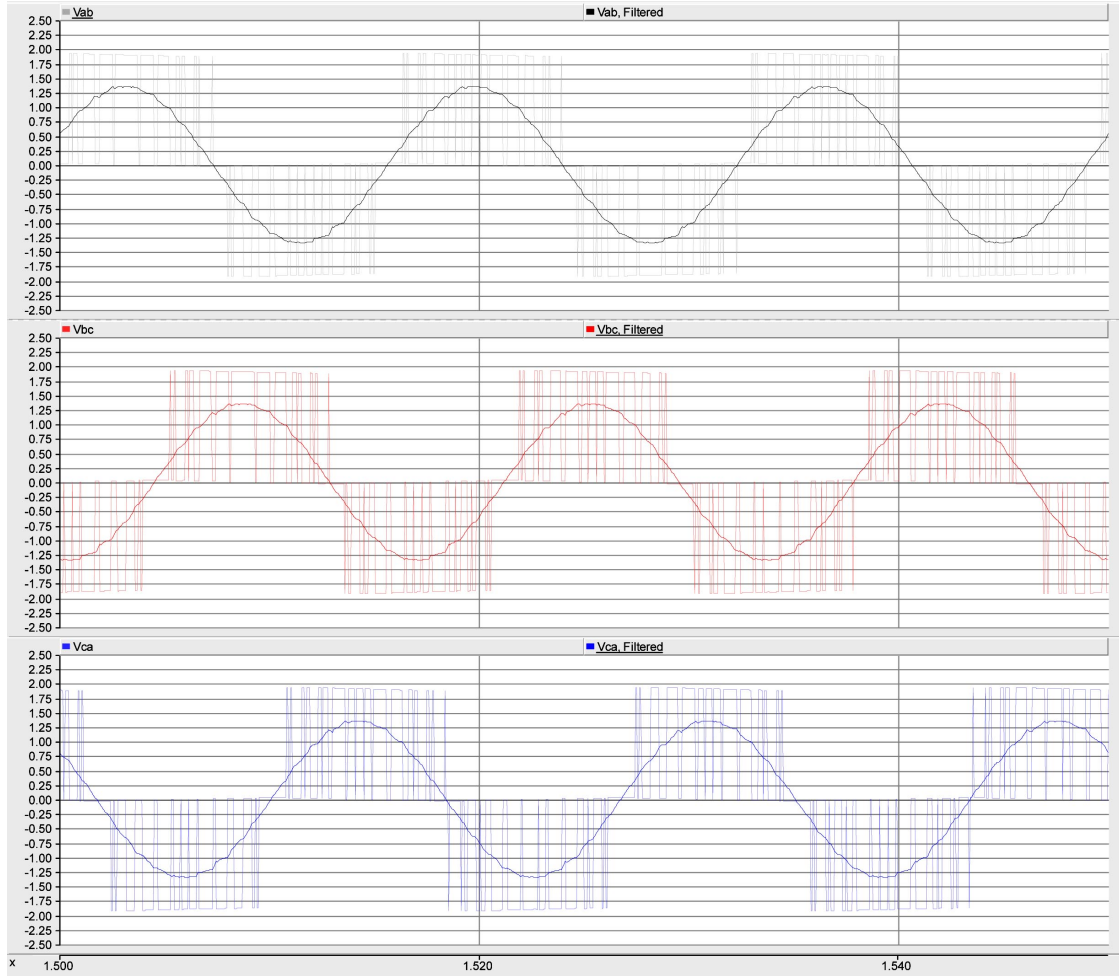


Figure 4.15 Input and Output Waveforms for Output Filter

#### 4.2.5 Internal Power Measurement

The D-STATCOM requires both active and reactive power measurement in order for the control system to function. To accomplish this, the Real/Reactive Power Meter component is used as shown in Figure 4.16.

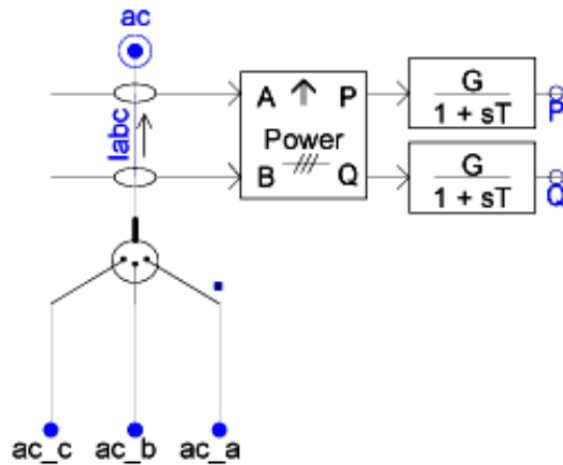


Figure 4.16 Internal Power Measurement Implementation

The Real/Reactive Power Meter measures data from two Node Loops to calculate both real and reactive power. The two nodes must be separated by any series-connected component. For this model, a simple three-phase ammeter is used to separate the two nodes. The meter then outputs both the active and reactive power measured in MW and Mvar, respectively. The meter uses a smoothing time constant of 0.05 seconds.

### 4.3 Control Module

The control module uses the data from dc and ac voltage measurements, as well as from active and reactive power measurements, to control the magnitude and phase angles of the reference signals. This in turn controls the magnitude and phase angles of the output voltage waveform of the D-STATCOM. The control module consists of two sections: the dc voltage regulator and the ac voltage regulator.

#### 4.3.1 DC Voltage Regulator

The dc voltage regulator controls the voltage of the dc capacitor by changing the phase angles of the reference waveforms. It operates as a two-stage Proportional-Integral

(PI) controller that measures both dc bus voltage and active power transfer. A diagram of this control system can be seen in Figure 4.17.  $V_{PI}$  is the dc bus voltage. This signal, measured in kV, is provided from the top level of the system model and is passed through the D-STATCOM module to the control system. It is the feedback signal for the first stage of the regulator. It is subtracted from the set point of 2.0 kV to supply an error signal to the first PI stage. The output of this PI stage is then used as a set point for the second PI stage. The feedback signal for the second PI stage is the real power being supplied by the D-STATCOM, measured in MW. The output of the second stage then passes through a hard limiter to constrain the output to between -180 degrees and 180 degrees. Lastly, the output signal is split into three phase-specific signals so that phase A is equal to the output signal, phase B is equal to the output signal minus 120 degrees, and phase C is equal to the output signal plus 120 degrees. This three-signal array is then passed through an output port of the controller, which then goes to the SPWM generator.

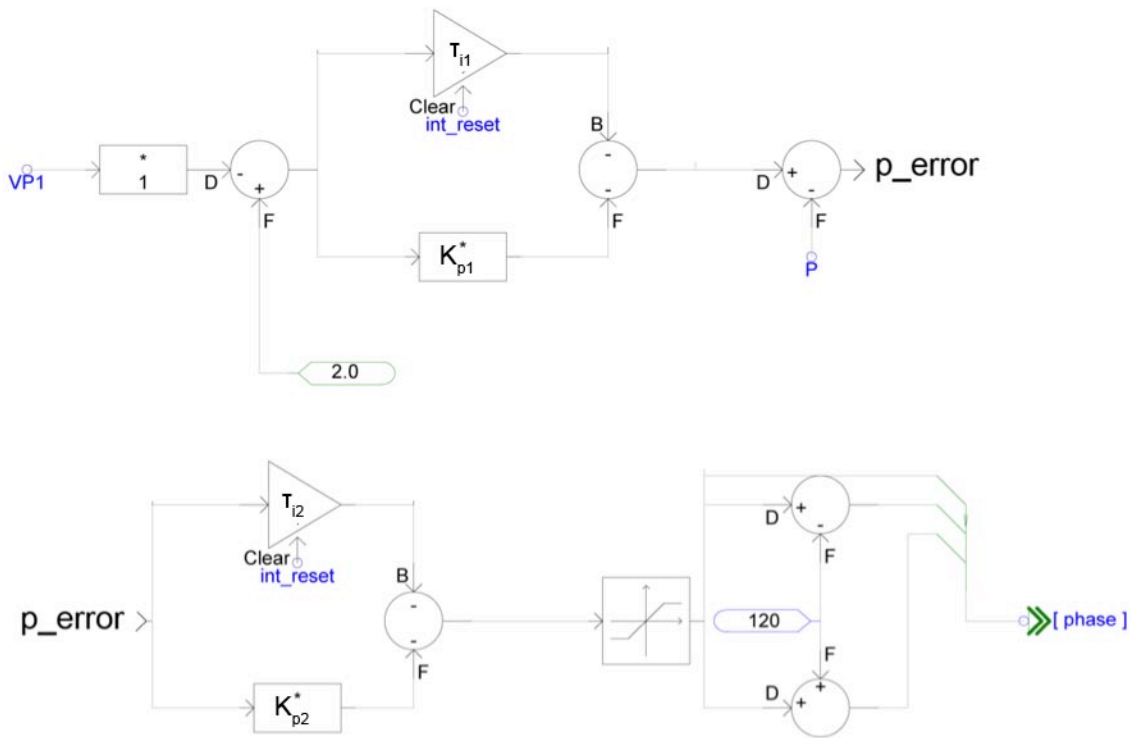


Figure 4.17 DC Voltage Regulator Diagram

The purpose of the dc voltage regulator is two-fold. Firstly, it maintains a constant dc voltage across the capacitor. Secondly, it keeps the real power transfer of the D-STATCOM as close to zero as possible. Both of these goals are achieved by controlling the phase angle of the D-STATCOM output. Tuning of the control system will be discussed in a later section.

### 4.3.2 AC Voltage Regulator

The ac voltage regulator controls the output voltage of the D-STATCOM by controlling the amplitudes of the reference waveforms. Controlling the output voltage of the D-STATCOM directly controls reactive power delivered, which in turn directly controls the voltage at the PCC. This can be explained by using Equation ( 2.2 ). As reactive power delivered by the D-STATCOM increases while the load remains constant,

the reactive power delivered by the grid decreases. Because the grid supply voltage is held constant, the voltage at the PCC will rise.

The topology for the ac voltage regulator is similar to that of the dc voltage regulator. A two-stage PI controller measures the voltage of the PCC and the reactive power delivered by the D-STATCOM and uses this information to control the magnitude of the reference waveform. A diagram of this control system can be seen in Figure 4.18.  $V_{grid}$  is the three-phase rms voltage seen at the PCC, measured in per-unit with a base value of 12 kV. It is measured at the top level of the system model and passed through the D-STATCOM module to the control module. It is the feedback signal for the first stage of the control system. It is subtracted from the set point of 1.0 pu to supply the error signal for the first stage of the control system. This error signal then passes through the first PI controller to create the reactive power set point. The measured reactive power delivered by the D-STATCOM is then subtracted from this output to create the reactive power error signal. This signal goes through a second PI controller to create a magnitude signal. This signal is then hard-limited to stay within values of zero and one, smoothed with a real pole filter, and then passed through an output port of the control module to the SPWM generator.

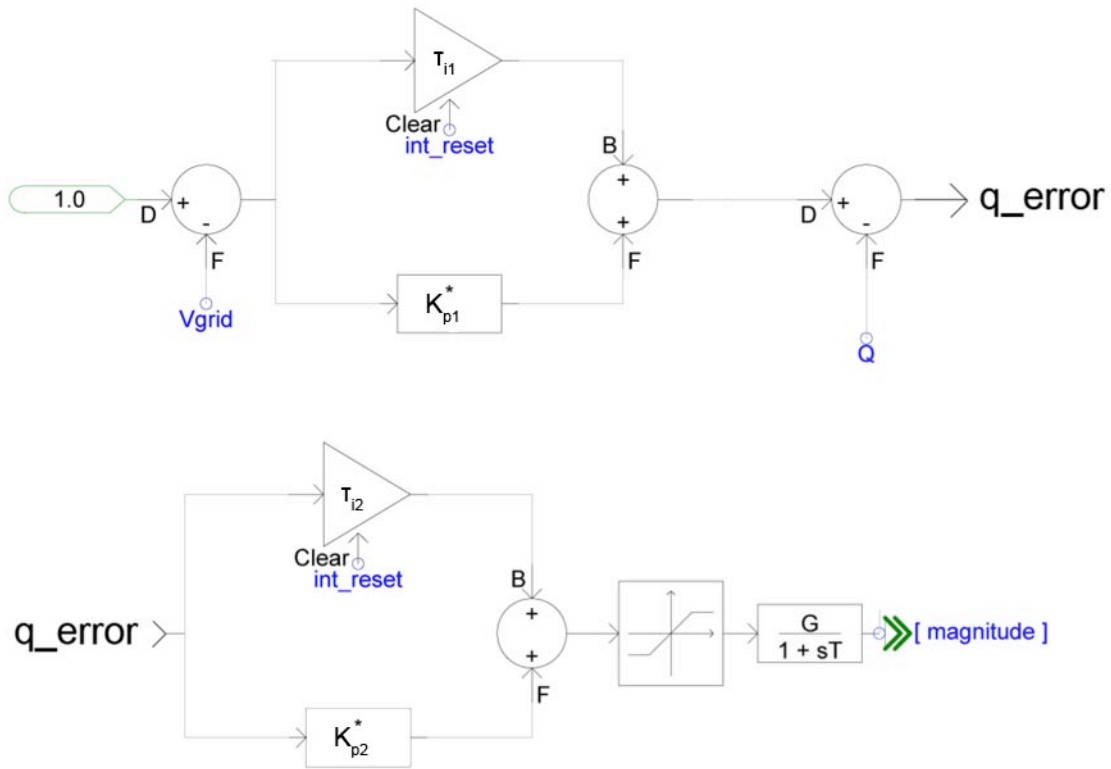


Figure 4.18 AC Voltage Regulator Diagram

#### 4.4 Control Module Tuning

Tuning of the control module is challenging because four measured parameters are used to control two separate processes, both of which affect the operation of the other process. Furthermore, several of the measurements are modified with smoothing filters, which also has a significant effect on the control system. Thus, there are many parameters that can be modified, and all of the parameters affect several performance characteristics to varying degrees.

The D-STATCOMs should maintain stability when both units are operating in parallel. They should also remain stable when a large load is brought online, resulting in the D-STATCOMs supplying their maximum reactive power output. With these

conditions in mind, a test case is created that simulates operation with these conditions. The initial conditions for this case are as follows:

- Both dc breakers closed
- Both load breakers open
- Both D-STATCOM ac breakers open
- Both feedback rectifier breakers open
- Grid supply breaker closed
- Both D-STATCOMs are turned off

These conditions connect only the grid supply to the PCC, resulting in a measured PCC voltage of approximately 1.0 per unit. These conditions remain for 0.2 seconds. Then, the D-STATCOM ac breakers are turned on. After 0.5 seconds, both D-STATCOMs are turned on, causing the control systems to operate and resulting in the dc capacitors charging to approximately 2.0 kV. At 1.0 seconds, load breaker 1 closes, bringing the 1.0 MW + 1.7 Mvar load online. At 2.0 seconds, load breaker 1 opens. These time values were chosen because they allow enough time for the system to reach steady state while keeping simulation times reasonably low. They also allow for the full-load and no-load step responses to be measured.

#### **4.4.1 Measurement Smoothing Time Constants**

Measurement values are the basis of the control system, so generating adequate measurement signals is essential to the operation of the D-STATCOM.

The ac voltage at the PCC is measured with the three-phase rms meter using a digital topology. According to PSCAD documentation, the digital topology produces a



smooth output signal that is appropriate for control systems. The meter is configured to take 128 samples per cycle. Base voltage is 12 kV and frequency is 60 Hz. The resulting signal has minimal ripple but still responds quickly to changes in voltage.

As described previously, the active and reactive power measurements include smoothing time constant values of 0.05 seconds, implemented as a real pole filter. These time constants are chosen because it is the smallest value that minimizes ripple while still allowing for reasonable response time. The effect of various smoothing time constants on the reactive power measurement can be seen in Figure 4.19.

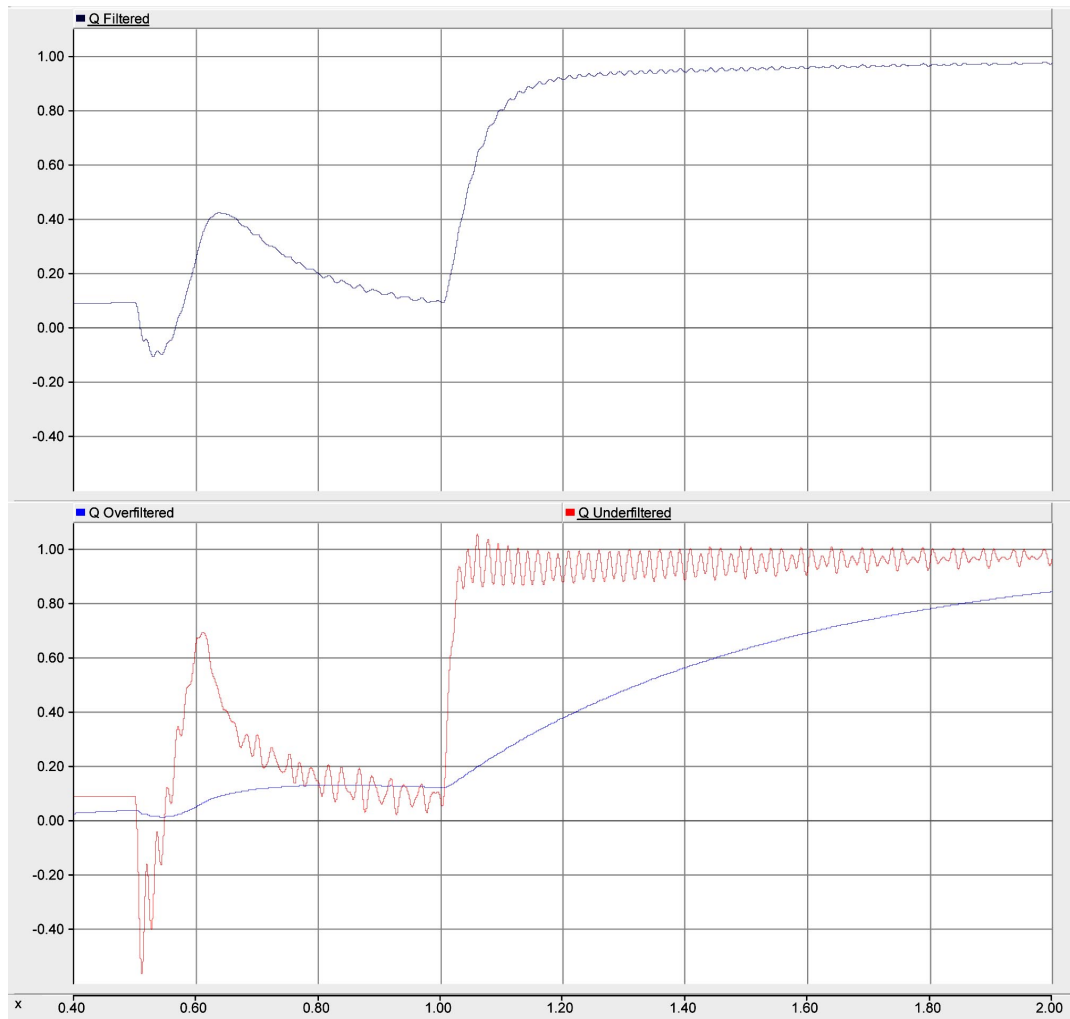


Figure 4.19 Reactive Power Measurement Signal with Various Smoothing Time Constants

The dc voltage measurement is filtered by a real pole filter. The dc capacitor is sized to minimize voltage ripple, but ripple still can occur during transient events. A real pole filter with a time constant of 0.02 is used to minimize the ripple while still resulting in fast response times. An example of the effect of filtering the dc voltage signal can be seen in Figure 4.20.

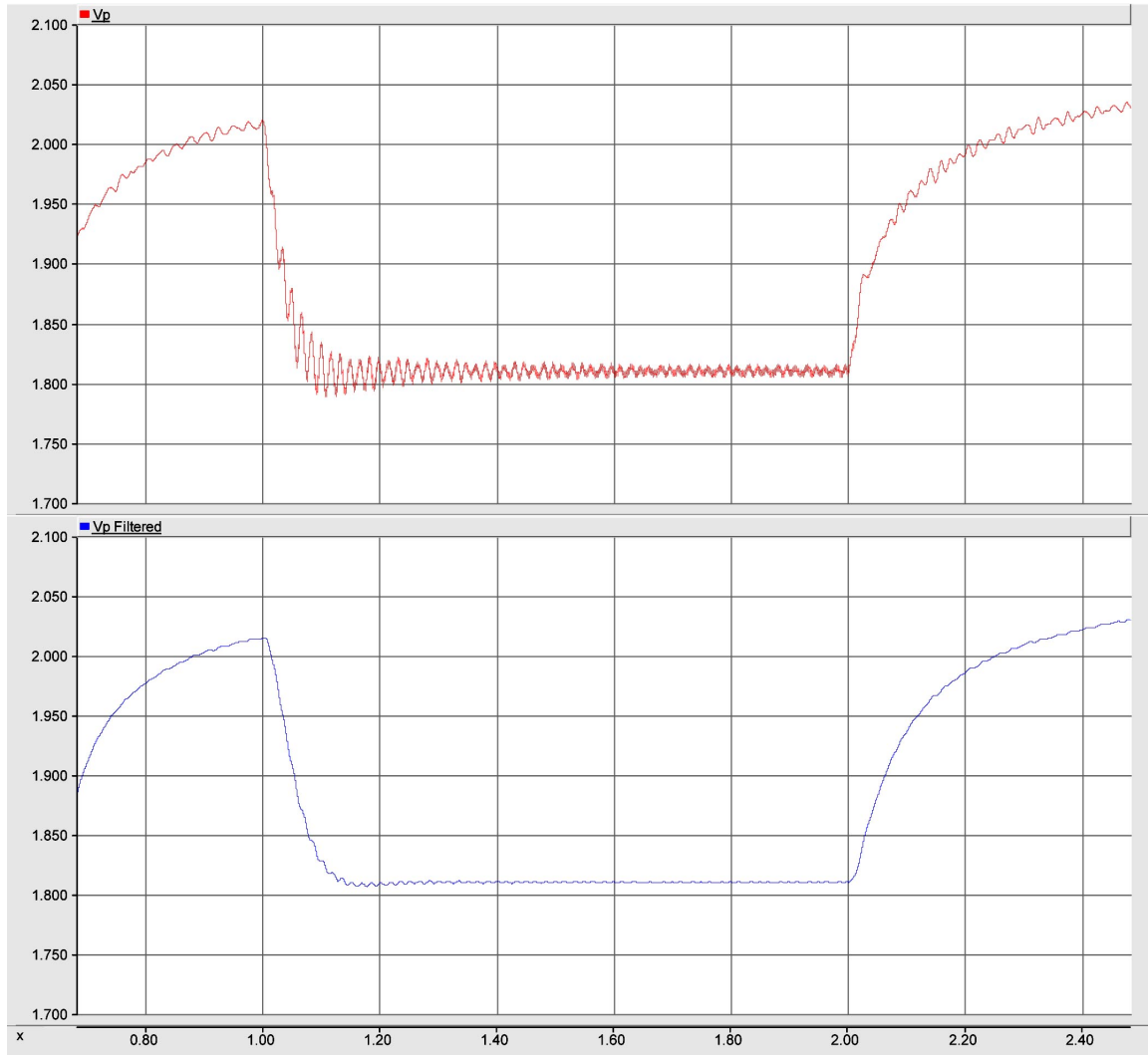


Figure 4.20 Unfiltered (top) vs. Filtered (bottom) DC Voltage Signals

#### 4.4.2 AC Voltage Regulator Tuning

The ac voltage regulator is the first control system to be tuned. To tune the system, the dc capacitor is removed from the system and replaced with a constant dc voltage source of 2.0 kV so that the un-tuned dc voltage regulator does not affect the system. An additional modified test case is also used. In addition to the 1.0 MW + 1.7 Mvar load that is used in the normal test case, a second test case with a 0.5MW + 0.5 Mvar load is also used to simulate a scenario where the D-STATCOMs are operating at less than full load.

This allows the ac voltage regulator to be tuned to both full load and partial load conditions.

An iterative method is used to determine the parameters for the control system. All proportional constants are initially set to unity. All integral time constants are initially set to 10 so that the integral term has a minimal effect on the system. Next, the first iteration measurements are taken by running the test case with a 0.5MW + 0.5 Mvar load. Both full load PCC voltage measurements and no load PCC voltage measurements are taken. Both measurements should ideally be 1.0 pu. The first several steps in the iteration aim to achieve 1.0 pu for both these measurements without regard to response time. Proportional constants are increased and integral time constants are decreased until 1.0 pu is achieved, as seen in Table 4.1.

The last tuning iterations are intended to improve the response time of the system while maintaining stability and preventing oscillations. This is done by decreasing the integral time constants until overshoot occurs. The smallest time constants that do not result in overshoot are the chosen time constants for the control system. Two example plots are shown in Figure 4.21 and Figure 4.22.

Table 4.1 Selected AC Voltage Regulator Tuning Coefficients and Measurements

$K_{p1}$	1	2	5	5	5	5	5	5
$K_{p2}$	1	1	1	1	1	1	1	1
$\tau_{i1}$	10	1	0.5	0.1	0.1	0.02	0.005	0.003
$\tau_{i2}$	10	1	1	1	0.1	0.1	0.1	0.05
<b>Full Load PCC Voltage (pu)</b>	0.9239	0.9476	0.9626	0.9778	0.9837	1.0003	1	1.0005
<b>No Load PCC Voltage (pu)</b>	0.9758	0.9775	0.9823	0.9884	0.9955	1.0041	1.0032	1.0007

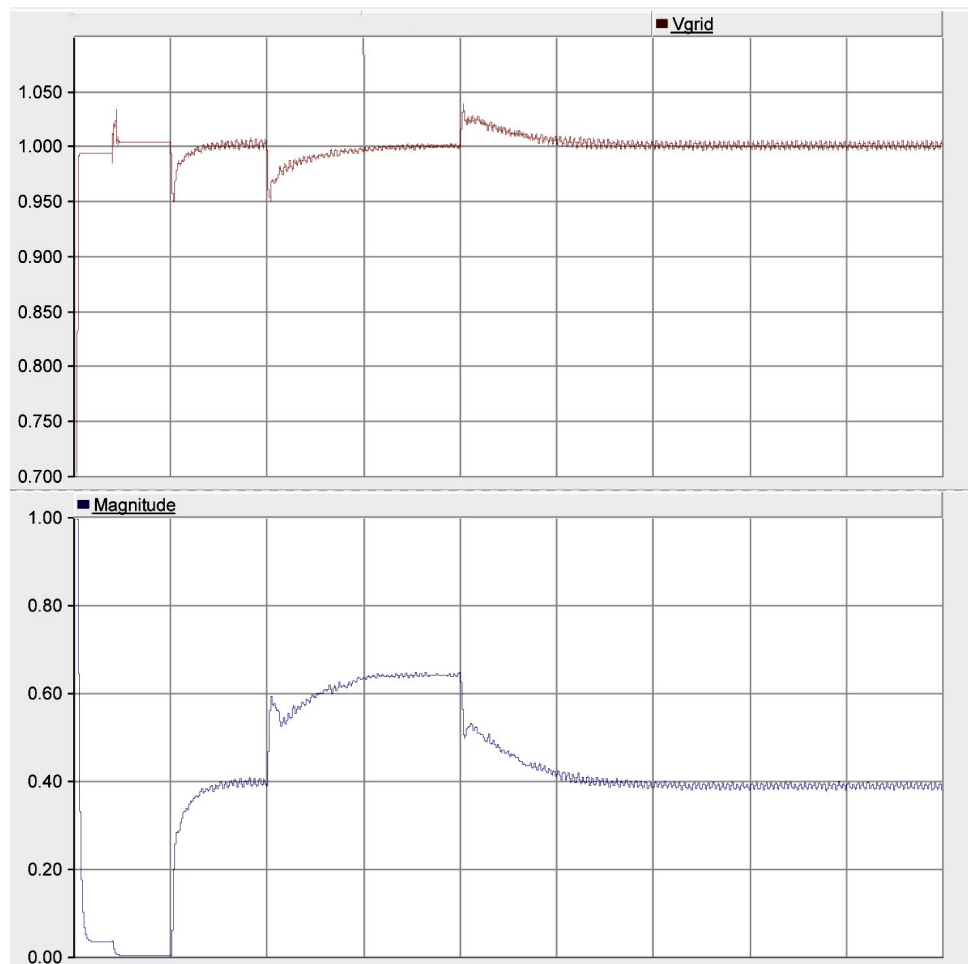


Figure 4.21 PCC Voltage and SPWM Magnitude, Case 1 (0.5 seconds per x-division)

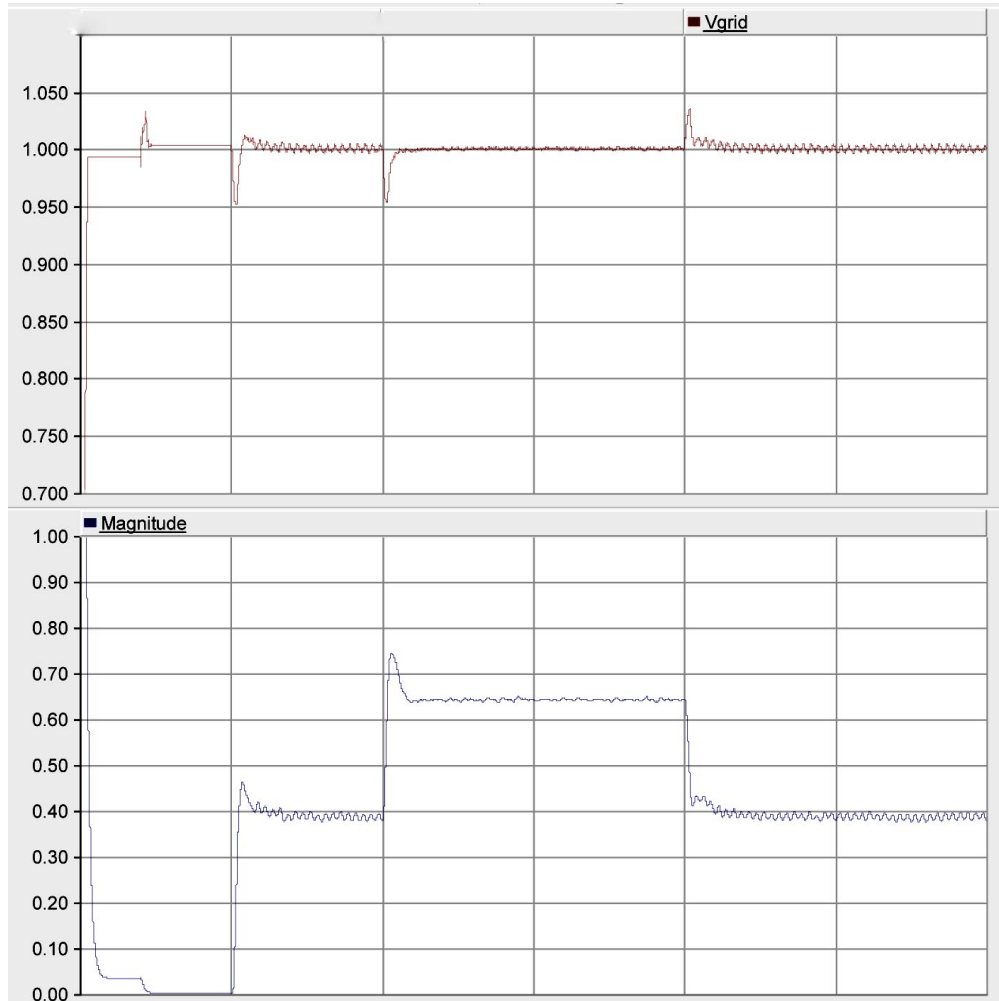


Figure 4.22 PCC Voltage and SPWM Magnitude, Case 2 (0.5 seconds per x-division)

Figure 4.21 shows the PCC voltage and SPWM magnitude for  $K_{p1} = 5$ ,  $K_{p2} = 1$ ,  $\tau_{i1} = 0.02$ , and  $\tau_{i2} = 0.1$ . The PCC voltage, reaches the ideal value of 1.0, but it reaches this value after approximately 0.5 seconds after the load condition changes. The system must be able to respond quicker, and Figure 4.22 shows the result of decreasing the integral time constants in order to improve the response time. For Figure 4.22,  $\tau_{i1} = 0.005$ , and  $\tau_{i2} = 0.05$ . The response time to the change in load condition is less than 0.1 seconds and the system remains stable.

After the parameters are determined for the 0.5MW + 0.5 Mvar load, the test is repeated with the 1.0 MW + 1.7 Mvar load to ensure that the D-STATCOMs quickly supply their maximum rated reactive power. At this point, tuning of the ac voltage regulator is complete, the dc voltage sources are removed, and the dc capacitors are replaced. The final parameters for the ac voltage regulator are as follows:  $K_{p1} = 5$ ,  $K_{p2} = 1$ ,  $\tau_{i1} = 0.003$ , and  $\tau_{i2} = 0.05$ .

#### **4.4.3 DC Voltage Regulator Tuning**

An iterative approach is also used to tune the dc voltage regulator. Only the 1.0 MW + 1.7 Mvar load is used to tune the dc voltage regulator and the ac voltage regulator is left in place with the parameters determined in Section 4.4.2. Both integral time constants are initially set to 10 so their effect on the output is minimal. The proportional constants for both stages are also set to unity. The first iteration measurements are then taken. No-load and full-load dc voltage measurements are taken. The ideal value for both measurements should be 2.0 kV. After this, proportional coefficients and integral time constants are decreased until the steady-state dc voltage reaches 2.0 kV for both no-load and full-load conditions. The dc voltage response of an early iteration of the tuning process is shown in Figure 4.23. At this iteration,  $K_{p1} = 40$  and  $\tau_{i1} = 0.25$ . Note the undervoltage condition for full load and the overvoltage condition for no load.

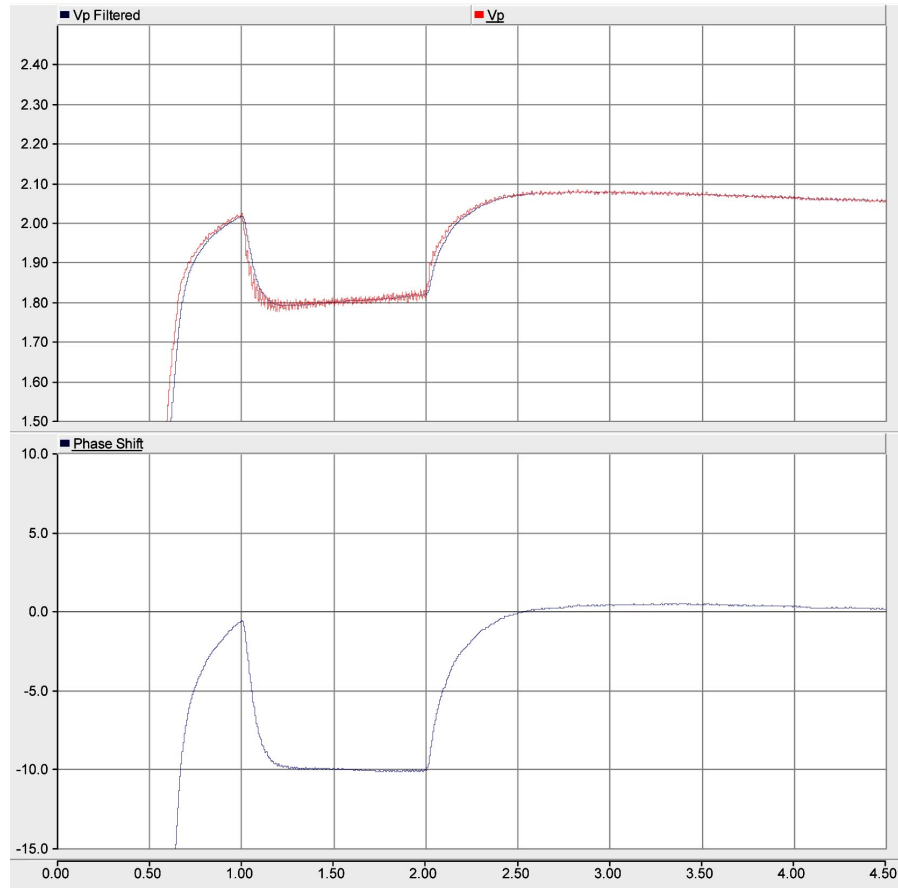


Figure 4.23 DC Voltage Response For  $K_{p1} = 40$  and  $\tau_{i1} = 0.25$

After preliminary coefficients are determined, the integral time constants are further decreased to improve response time. During this step, it is evident that the second stage of the control system is unnecessary for achieving the required dc voltage and response time. The second stage compares the real power transfer to the output of the first stage. Because there are no components in the D-STATCOM that can source or sink a significant amount of real power, real power transfer tends to remain very low and thus the error signal for the second stage is approximately equal to the output of the first stage. This can be seen in Figure 4.24. Thus, the second stage of the control system is removed.



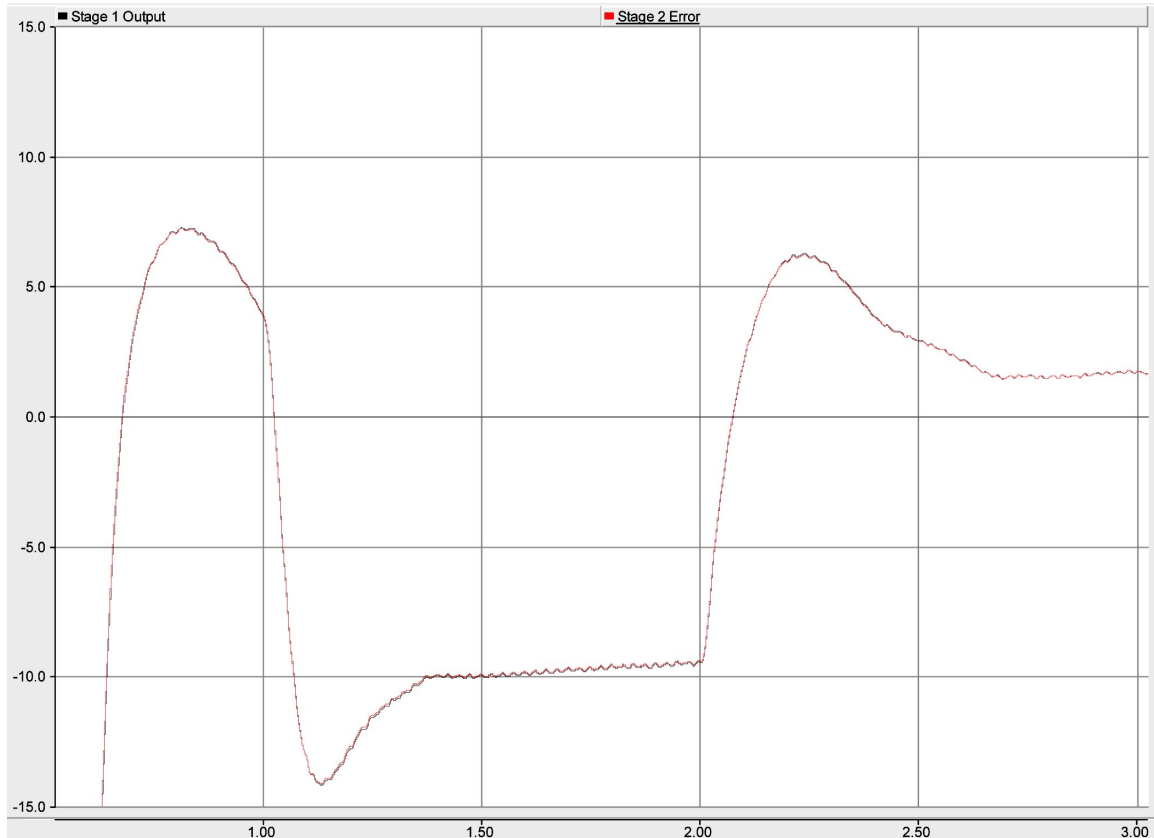


Figure 4.24 DC Voltage Regulator Stage 1 Output vs. Stage 2 Error

In the late iterations of the tuning process, it is evident that the integral term improves the response time of the dc voltage regulation after the dc capacitor has been initially charged, but when the D-STATCOM is initially brought online, the integral term causes excessive overshoot of the dc voltage, as shown in Figure 4.25. For this iteration,  $K_{p1} = 70$  and  $\tau_{i1} = 0.002$ . Note the peak dc voltage of nearly 2.7 kV during the initial charging period. The same iteration is shown with a hard limit of  $\pm 10$  on the integral term in Figure 4.26. The dc voltage response of the system remains the same as it was without the limit, but the peak dc voltage during the initial charging period is reduced to 2.15 kV. Thus, a hard limit of  $\pm 10$  is included in the integral term of the dc voltage regulator control system.

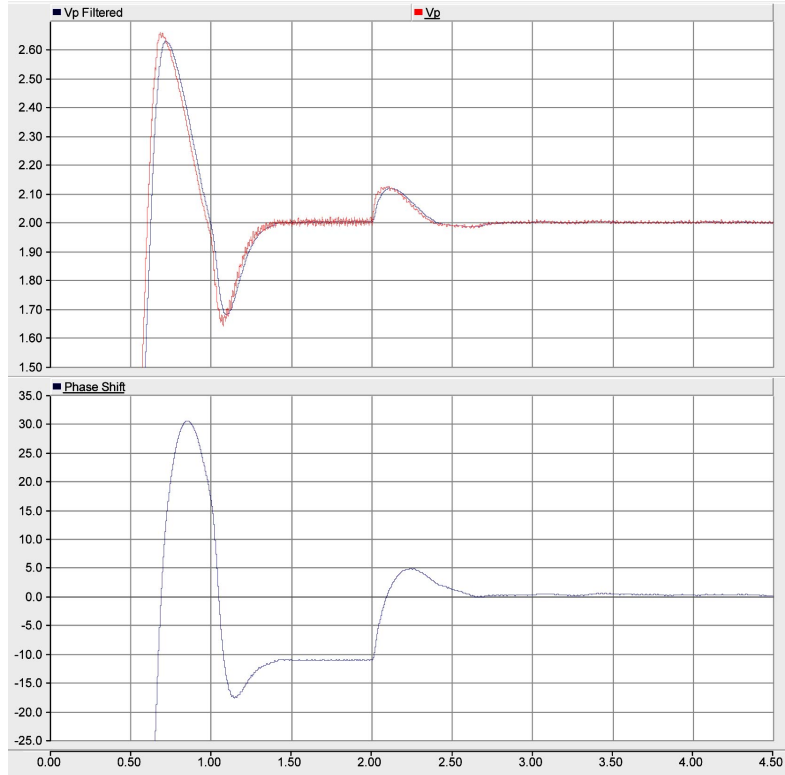


Figure 4.25 DC Voltage Response Without Integral Limit

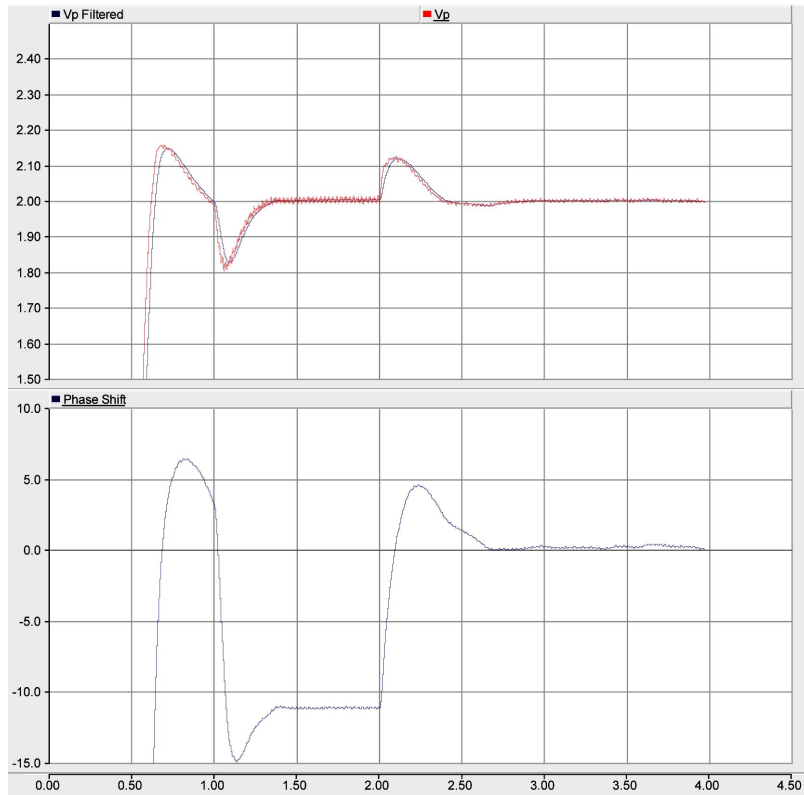


Figure 4.26 DC Voltage Response with Integral Limit

At this point, tuning is complete. Coefficients and measurements from several of the iterations are shown in Table 4.2. The final parameters for the ac voltage regulator are as follows:  $K_{p1} = 70$  and  $\tau_{i1} = 0.002$ .

Table 4.2 Selected DC Voltage Regulator Tuning Coefficients and Measurements

<b>Kp1</b>	1	10	20	40	50	70	70
<b>Kp2</b>	1	1	1	1	-	-	-
<b><math>\tau_{i1}</math></b>	10	1	0.5	0.25	0.1	0.007	0.002
<b><math>\tau_{i2}</math></b>	10	10	10	10	-	-	-
<b>Full Load DC Voltage (kV)</b>	0.641	1.407	1.627	1.791	1.874	1.996	1.984
<b>No Load DC Voltage (kV)</b>	1.576	2.218	2.131	2.075	2.063	2	2

## 5 Testing and Results

The performance analysis of the D-STATCOMs is based on several parameters. Among these parameters are PCC voltage, response time, THD, and dc capacitor voltage. These parameters are also measured in several configurations, including single unit operation, synchronous dual unit operation, and asynchronous dual unit operation. Two different loads are used: a 1.7 MW + 1.0 Mvar load and a 0.5 MW + 0.5 Mvar load. The 1.7 MW + 1.0 Mvar load is the primary load used for testing.

### 5.1 Full Load With No Regulation

Before testing the performance of the D-STATCOMs, a control case is tested to measure the response of the PCC to the 1.7 MW + 1.0 Mvar load. In this test case, the load is initially offline. At 1.0 seconds, the load is brought online. At 2.0 seconds, the load is brought offline again. The voltage of the PCC is measured and the results are provided in Table 5.1. A plot of the PCC voltage is shown in Figure 5.1.

Table 5.1 Measured Values, Full Load, No Regulation

<b>PCC Steady State Full Load Voltage (pu)</b>	<b>Full Load Response Time (ms)</b>	<b>No Load Response Time (ms)</b>	<b>Full Load THD</b>	<b>No Load THD</b>
0.8491	200	17	0	0

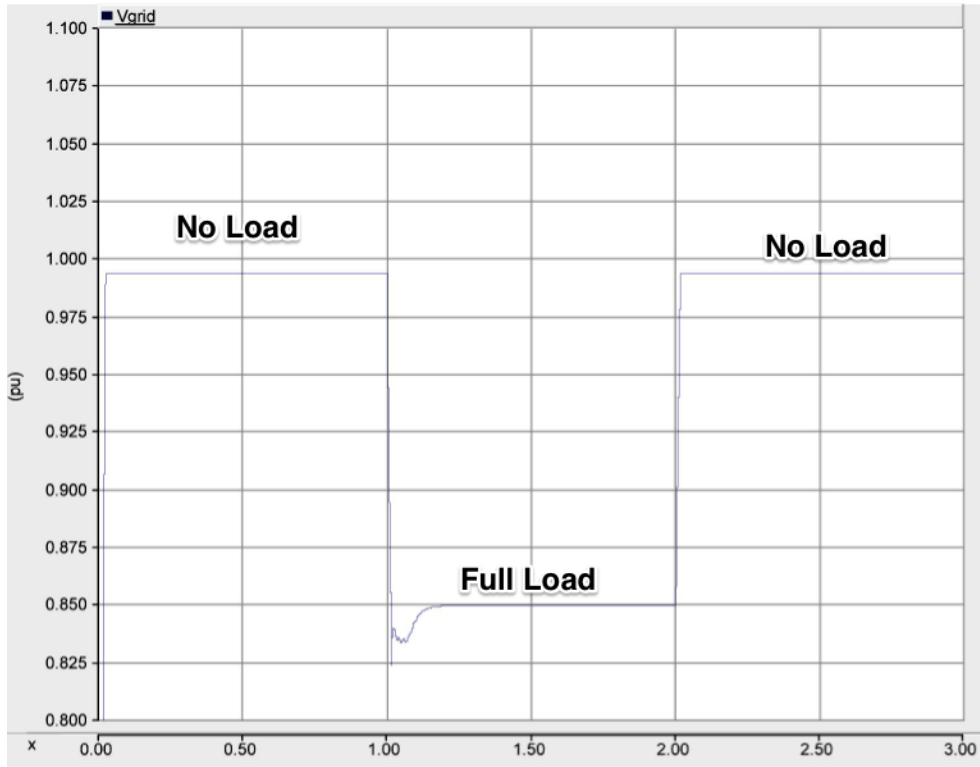


Figure 5.1 PCC Voltage, Full Load, No Regulation

The response time is relatively high when the load is brought online because of the way that the fixed load calculates the resistance and reactance values of its load. Because the load is initially separated from the PCC, no voltage is seen across the load and the calculated resistance and reactance values are not correct for the PCC voltage. As soon as the load is brought online, the fixed load recalculates the resistance and reactance values until the correct active and reactive power is dissipated.

The steady state PCC voltage at full load is 0.8491 pu, which is quite low. The D-STATCOMs will improve this voltage significantly.

## 5.2 Single D-STATCOM Operation

The first tests conducted with the D-STATCOM are single-unit tests. Single-unit tests allow the performance of the D-STATCOM to be characterized without

confounding interactions with the other D-STATCOM. These tests also facilitate analysis of the operation of the parallel full-wave rectifier. Two test cases are conducted using a single D-STATCOM. One test case characterizes the operation of the D-STATCOM with the parallel full-wave rectifier and the other case does not include the parallel full-wave rectifier. In addition to these two test cases, power loss analysis is also performed on a single unit to characterize the effect of different reactive power output levels on power loss, as well as to characterize the effect of the parallel rectifier on power loss.

### 5.2.1 Single Operation without Parallel Rectifier

For the test case that omits the parallel rectifier, both the load and the D-STATCOM are initially disconnected. At 0.2 seconds, the ac side of the D-STATCOM is brought online, but the D-STATCOM is not operational. At 0.5 seconds, the D-STATCOM is turned on. At 1.0 seconds, the 1.7 MW + 1.0 Mvar load is brought online. At 3.0 seconds, the load is taken offline. Results from this test are shown in Table 5.2.

Table 5.2 Measured Values, Single Operation without Parallel Rectifier

<b>PCC Steady State Full Load Voltage (pu)</b>	<b>Full Load Response Time (ms)</b>	<b>No Load Response Time (ms)</b>	<b>Full Load THD</b>	<b>No Load THD</b>
0.9096	309	291	0.99%	1.92%
<b>P supplied by D-STATCOM under full load(MW)</b>	<b>Q supplied by D-STATCOM under full load (Mvar)</b>	<b>Full load dc capacitor voltage (kV)</b>	<b>Inrush Current (kA)</b>	<b>dc voltage ripple (kV)</b>
-0.058	1.003	2	2.15	0.01

The PCC steady state voltage improved by 0.0605 pu versus the unregulated case. Full-load response time and no-load response time are 309 ms and 291 ms, respectively. These times are measured from the time the load changes to the time that the PCC voltage reaches its steady state value. For the full-load response time, the steady state voltage is 0.9096 pu, and for the no-load response time, the steady state voltage is 1.00 pu. The response time can be improved by using more aggressive tuning constants, but this has a negative effect on the PCC voltage when the D-STATCOM is initially brought online. Figure 5.2 shows the PCC voltage response for this test.

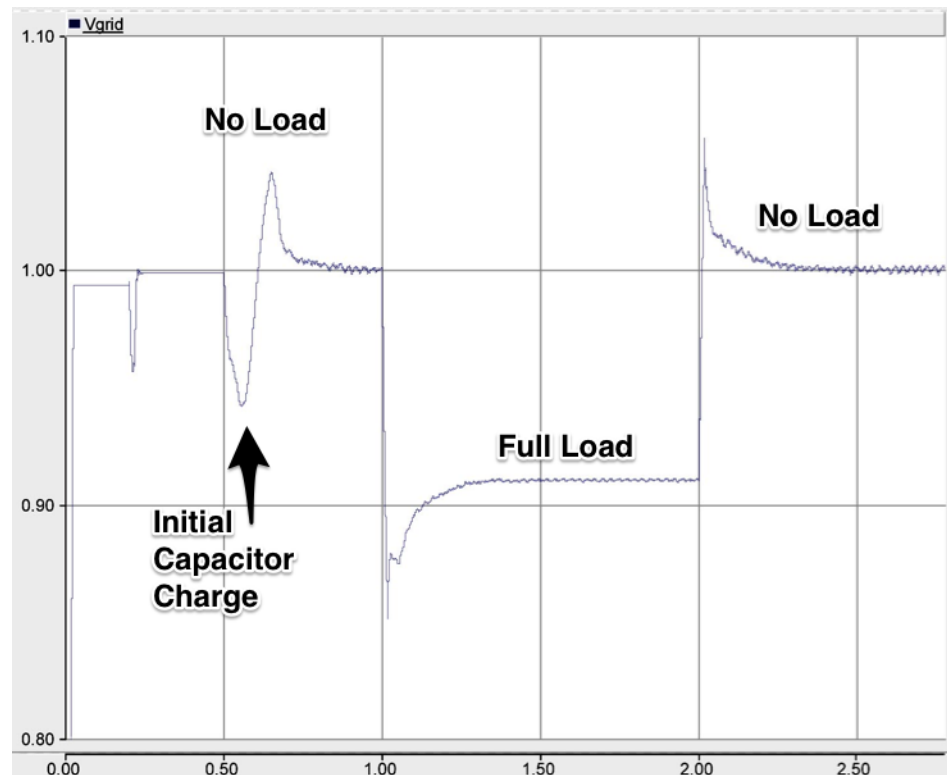


Figure 5.2 PCC Voltage, Single Operation without Parallel Rectifier

As can be seen in Figure 5.2, there are several fluctuations in PCC voltage throughout the test. The first fluctuation occurs at 0.2 seconds when the ac circuit breaker for the D-STATCOM is closed, allowing the dc capacitor to charge from zero volts to the

dc voltage of the full-wave rectifier. This results in a brief period of low impedance connected in shunt to the PCC, bringing its voltage down. The three-phase inrush current at this period is shown in Figure 5.3. One phase experiences a peak inrush current magnitude of 2.15 kA, while the other phases have peak inrush currents of around 1 kA. The inrush current oscillates at the initial closing of the circuit breaker because of the output filter's reaction to the effective step function created by the closing of the circuit breaker.



Figure 5.3 Inrush Current, Single Operation without Parallel Rectifier

At 0.5 seconds, the D-STATCOM IGBT bridge and control system is brought online. The control system causes the dc capacitor to charge to its steady-state value of



2.0 kV. This also causes a brief period of low impedance connected in shunt to the PCC, bringing its voltage down. Because adaptive tuning of the control system is not utilized in this model, the tuning of the control system must strike a balance between acceptable initial charging performance and reasonably quick response time to changes in load. Thus, an overshoot of the PCC voltage occurs during the initial charging of the dc capacitor to 2.0 kV.

At 1.0 second, the 1.7 MW + 1.0 Mvar load is brought online and the PCC voltage drops. The D-STATCOM reacts quickly to increase the voltage at the PCC. The PCC voltage is brought up to above 0.90 pu in less than 200 ms and then continues to rise to its steady state voltage. At 3.0 seconds, the load is taken offline resulting in a brief spike in PCC voltage as the D-STATCOM reacts to the change in load. The peak voltage spike is 1.055 pu and is quickly brought down to 1.0 pu.

### **5.2.2 Single Operation with Parallel Rectifier**

The test conditions for single operation with the parallel rectifier are the same as those of single operation without the parallel rectifier. Results for this test case are shown in Table 5.3.

Table 5.3 Measured Values, Single Operation with Parallel Rectifier

<b>PCC Steady State Full Load Voltage (pu)</b>	<b>Full Load Response Time (ms)</b>	<b>No Load Response Time (ms)</b>	<b>Full Load THD</b>	<b>No Load THD</b>
0.9097	309	291	1.05%	2.02%
<b>P supplied by D-STATCOM under full load(MW)</b>	<b>Q supplied by D-STATCOM under full load (Mvar)</b>	<b>Full load dc capacitor voltage (kV)</b>	<b>Inrush Current (kA)</b>	<b>dc voltage ripple (kV)</b>
-0.048	1.006	2.00	7.98	0.01

Results are very similar to the results for single operation without the parallel rectifier. The most notable difference is the significantly larger inrush current. The inrush current is 3.7 times larger than the inrush current for the previous test case. This is because the parallel rectifier has no inductance in series to slow the rate of rise of current, while the antiparallel diodes within the D-STATCOM are connected in series to the reactors used for the output filter. The inrush current is shown in Figure 5.4.

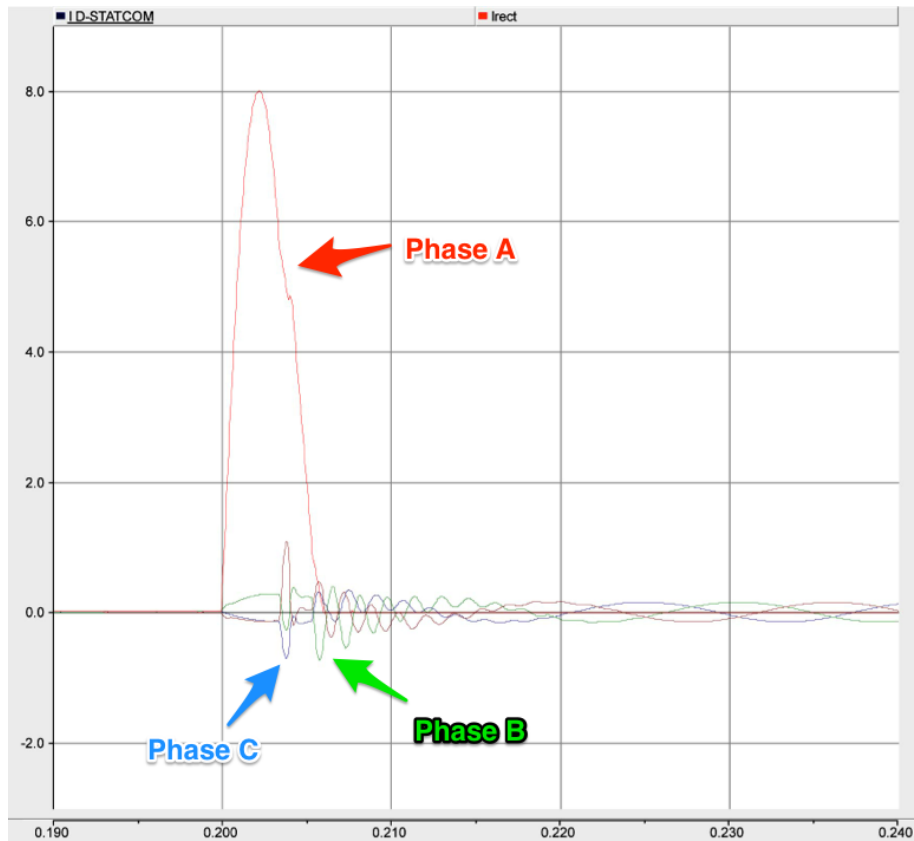


Figure 5.4 AC Inrush Current, Single Operation with Parallel Rectifier

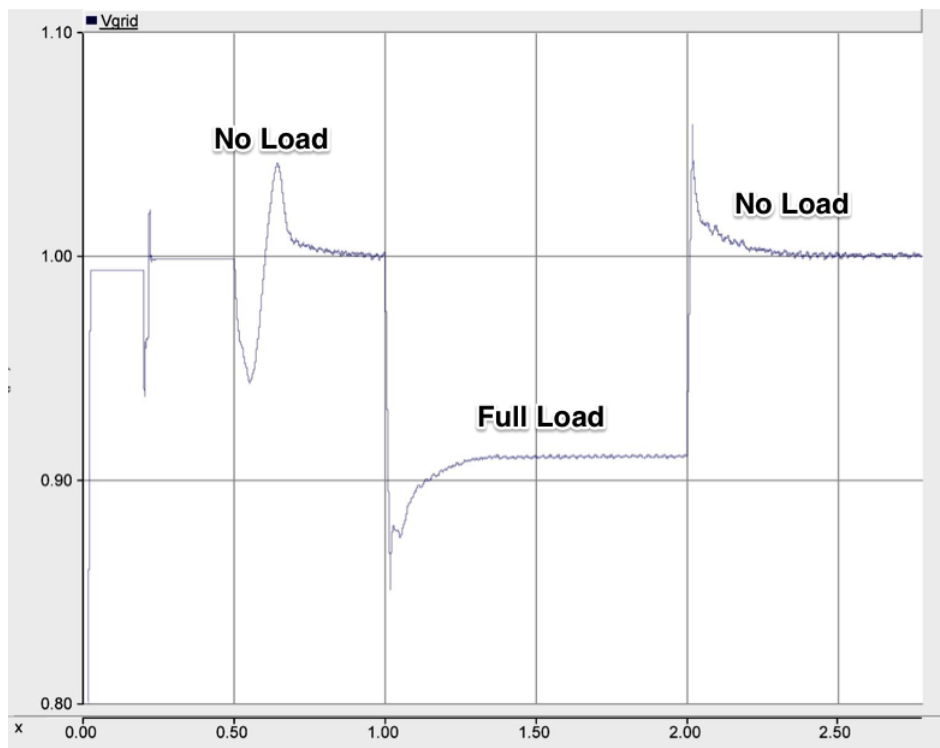


Figure 5.5 PCC Voltage, Single Operation with Parallel Rectifier

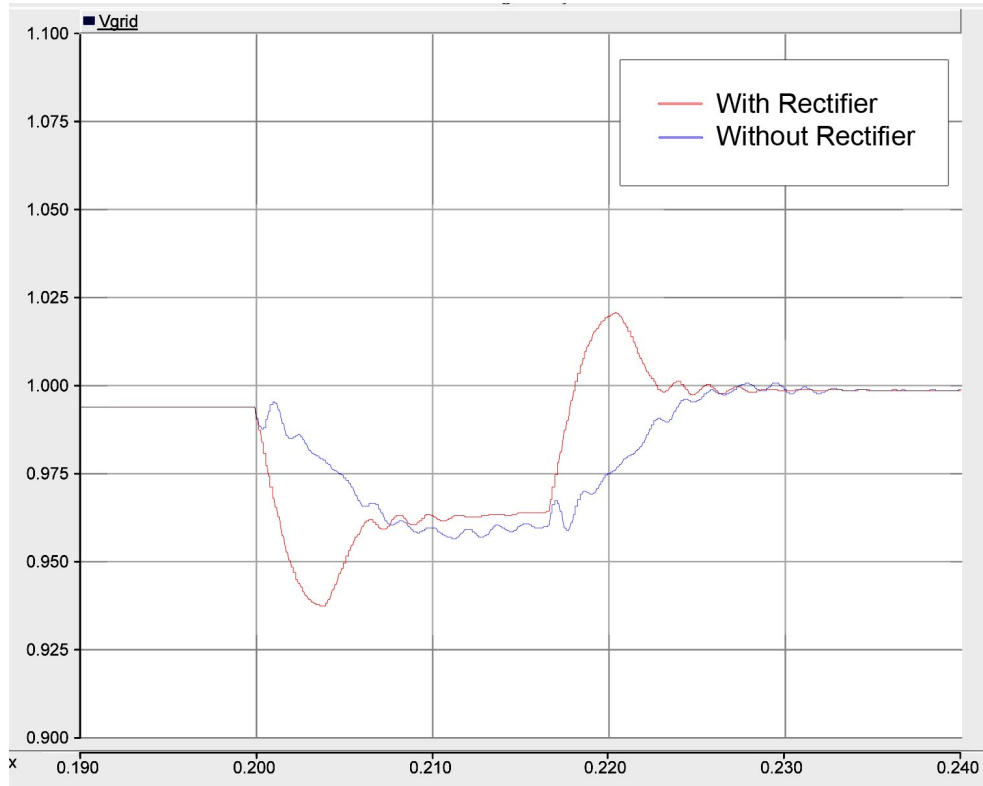


Figure 5.6 PCC Inrush Voltage, Single Operation with and without Parallel Rectifier

PCC voltage response is nearly identical to the previous test case, as shown in Figure 5.5. The only notable difference is the change in PCC inrush voltage. The inrush voltage profile for both cases is shown in Figure 5.6. The parallel rectifier causes the PCC voltage to drop to as low as 0.937 pu, while the PCC voltage drops to 0.960 pu without the parallel rectifier. This makes sense because the antiparallel diodes that are used to charge the capacitor are current-limited by the reactance of the output filter. This results in less of a voltage drop than when the parallel full-wave rectifier is used, since the rectifier has no current-limiting reactance. The PCC voltage also overshoots to 1.02 pu with the parallel rectifier.

DC ripple voltage during D-STATCOM operation is also measured for both test cases. If the ripple voltage is too high, the THD of the D-STATCOM may become

unacceptable. Furthermore, high ripple voltages can result in large  $\frac{dv}{dt}$ , which creates electromagnetic interference (EMI) [31]. DC ripple voltage for both tests can be seen in Figure 5.7 and Figure 5.8. The addition of the parallel rectifier does not significantly change the dc ripple voltage characteristics.

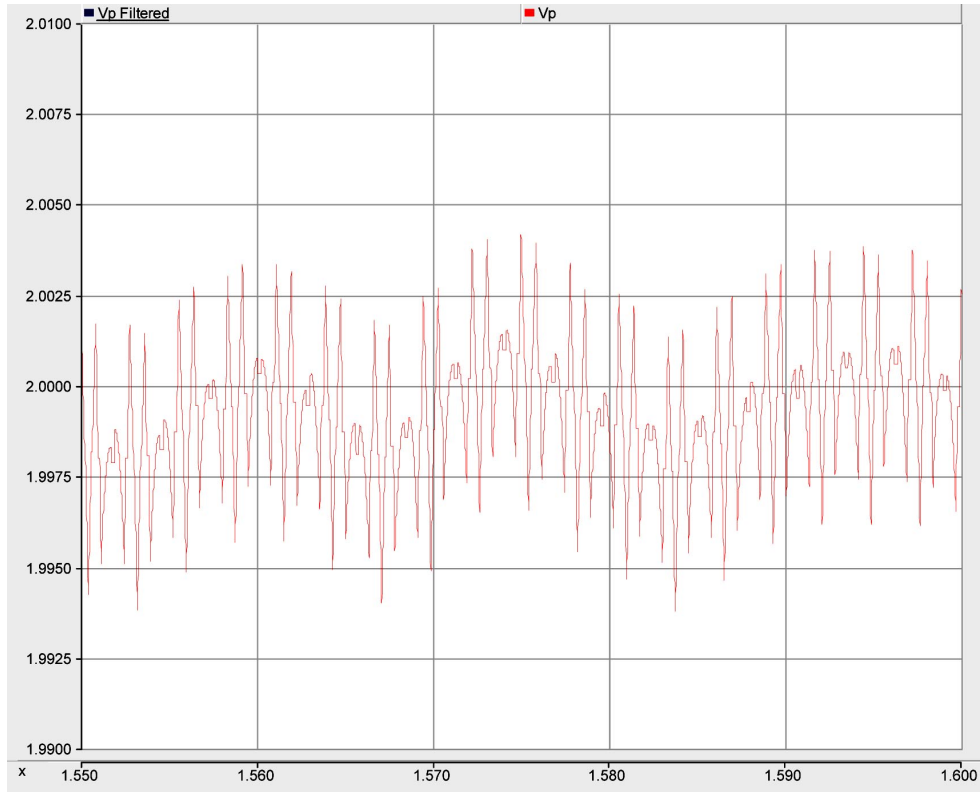


Figure 5.7 DC Ripple Voltage, Single Operation without Parallel Rectifier

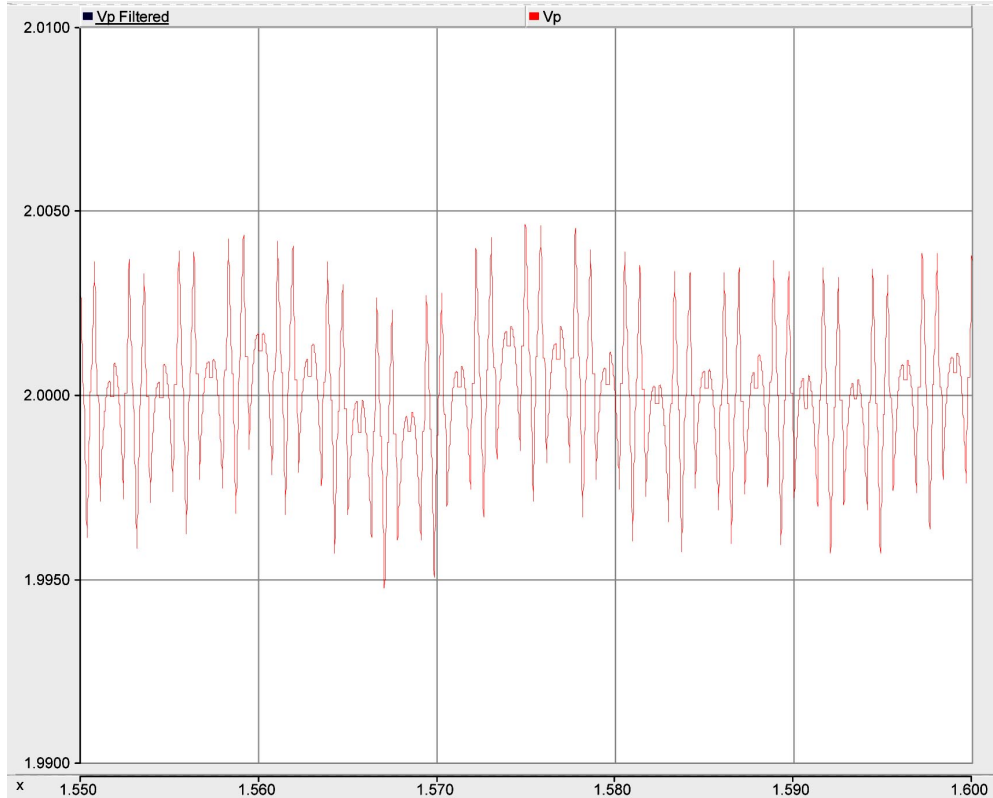


Figure 5.8 DC Ripple Voltage, Single Operation with Parallel Rectifier

### 5.2.3 Power Loss for Single D-STATCOM

In addition to measuring the step response characteristics of the individual D-STATCOM, steady state power loss is also analyzed both with and without the parallel rectifier at various reactive power levels. For this test, the PCC load is changed to achieve the desired reactive power output from the D-STATCOM. The real and reactive power drawn by the load are equal in magnitude for each respective reactive power output. Measured power loss values are shown in Figure 5.10.

Table 5.4 and are plotted in Figure 5.9.  $\frac{P_{Loss}}{Q_{Supplied}}$  ratios are shown in Table 5.5 and plotted in Figure 5.10.

Table 5.4 Measured Values, Power Loss for Single D-STATCOM

$Q_{\text{Supplied}}$ (Mvar)	0.0	0.2	0.4	0.6	0.8	1.0
$P_{\text{Loss}}$ Without Rectifier (kW)	16.33	16.34	19.28	26.45	36.15	52.68
$P_{\text{Loss}}$ With Rectifier (kW)	22.97	22.9	24.49	29.86	39.91	55.82

Table 5.5  $\frac{P_{\text{Loss}}}{Q_{\text{Supplied}}}$  for Single D-STATCOM

$Q_{\text{Supplied}}$ (Mvar)	0.0	0.2	0.4	0.6	0.8	1.0
$\frac{P_{\text{Loss}}}{Q_{\text{Supplied}}}$ Without Rectifier	-	0.0817	0.0482	0.0441	0.0452	0.0527
$\frac{P_{\text{Loss}}}{Q_{\text{Supplied}}}$ With Rectifier	-	0.1145	0.0612	0.0498	0.0499	0.0558

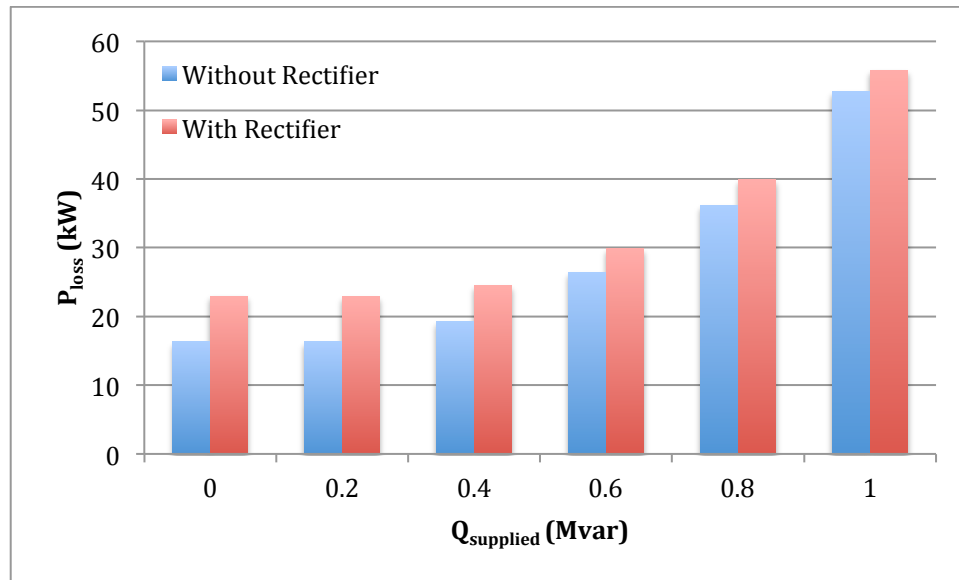


Figure 5.9  $P_{\text{loss}}$  vs.  $Q_{\text{supplied}}$

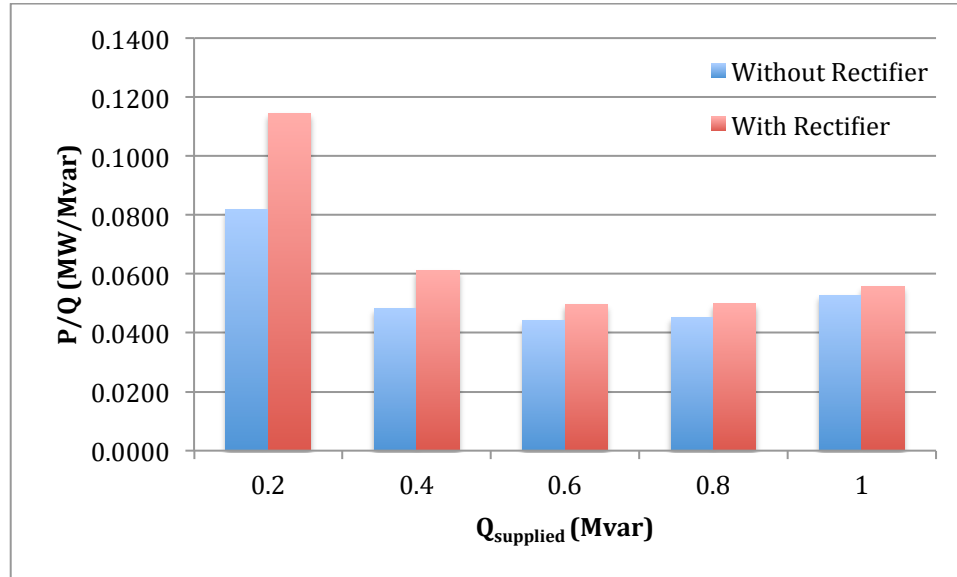


Figure 5.10  $\frac{P_{Loss}}{Q_{Supplied}}$  vs.  $Q_{supplied}$

On average, the addition of the parallel rectifier incurs an additional 4.79 kW of power loss. This power loss is more pronounced at lower reactive power levels.  $\frac{P_{Loss}}{Q_{Supplied}}$  is lowest at 0.6 Mvar of reactive power supplied. This ratio rises slightly for higher reactive power levels, and rises significantly for lower reactive power levels.

In single-unit operation mode, the D-STATCOM meets all of its design requirements. It supplies 1.0 Mvar to the PCC and produces an acceptable level of THD. The ac voltage waveform as measured from the PCC is sinusoidal with some slight distortion, as shown in Figure 5.11. The system remains stable during turn-on of the D-STATCOM unit, as well as during turn-on and turn-off of the load. However, the parallel rectifier has no apparent benefit for this test case. Most measured parameters are similar both with and without the parallel rectifier. Furthermore, the addition of the parallel rectifier caused much larger ac inrush current and a larger subsequent PCC inrush voltage drop, as well as greater power loss. Lastly, no theoretical or practical model of a



STATCOM or D-STATCOM presented in research includes a parallel rectifier. Thus, a parallel rectifier is unnecessary for the D-STATCOM operating in single-unit configuration.

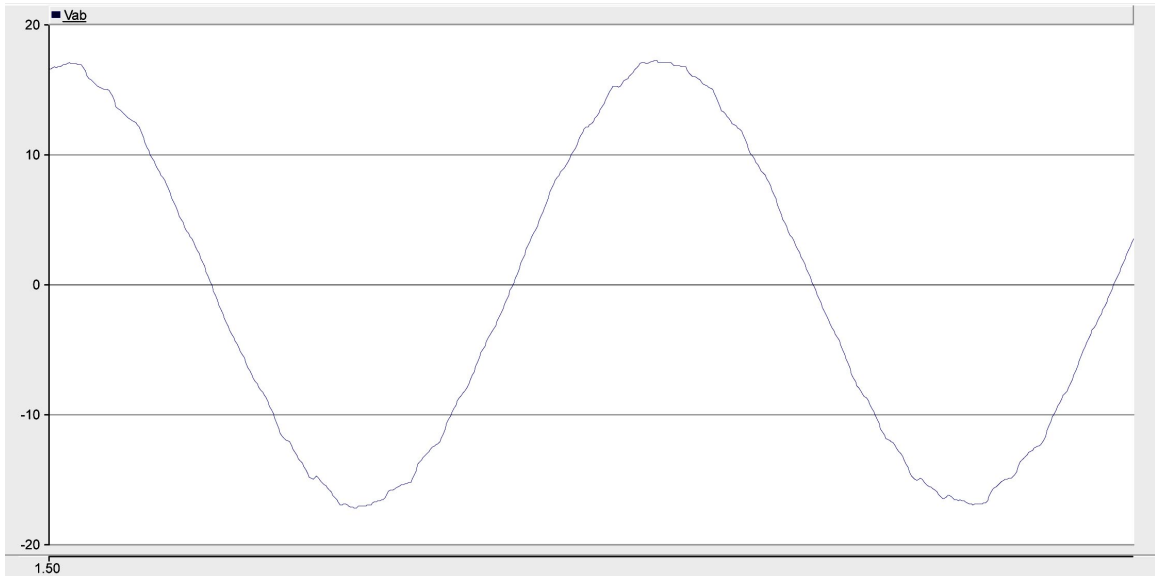


Figure 5.11 PCC Voltage Waveform With Single STATCOM Online

### 5.3 Synchronous Dual D-STATCOM Operation Without Initial Load

The following two tests are identical to the previous two tests, except two D-STATCOMs are used in parallel. Both D-STATCOMs are operated synchronously, i.e. they are both brought online at the same time. These test cases will confirm that the D-STATCOMs are able to remain stable when they are required to operate synchronously with each other.

#### 5.3.1 Synchronous Operation Without Parallel Rectifier

This test characterizes the operation of both D-STATCOMs when they are brought online with no parallel rectifier. The results are shown in Table 5.6.

Table 5.6 Measured Values, Synchronous Operation Without Parallel Rectifier

<b>PCC Steady State Full Load Voltage (pu)</b>	<b>Full Load Response Time (ms)</b>	<b>No Load Response Time (ms)</b>	<b>Full Load THD</b>	<b>No Load THD</b>
0.9655	325	294	1.46%	3.21%
<b>P supplied by D-STATCOM under full load(MW)</b>	<b>Q supplied by D-STATCOM under full load (Mvar)</b>	<b>Full load dc capacitor voltage (kV)</b>	<b>Inrush Current (kA)</b>	<b>dc voltage ripple (kV)</b>
-0.046	1.022	2	2.10	0.01

As expected, the full-load PCC voltage is higher than when only one D-STATCOM is operational. The full load PCC voltage is 0.0559 pu higher than for the single-unit test case. Response times are slightly slower because the steady-state voltage is higher. The THD values are also slightly higher because more total reactive power is being supplied from the D-STATCOMs.

Figure 5.12 plots the PCC voltage over time for this test case. The voltage profile is generally similar to that of the single-unit test case, however there are a few notable differences. Firstly, the initial voltage fluctuation when the D-STATCOM is brought online at 0.5 seconds is greater. The PCC voltage reaches a low value of 0.892 pu and a peak value of 1.065 pu during this period. Again, this voltage fluctuation can be significantly reduced if adaptive tuning of the control system is used to change the behavior of the D-STATCOM when it is initially brought online.

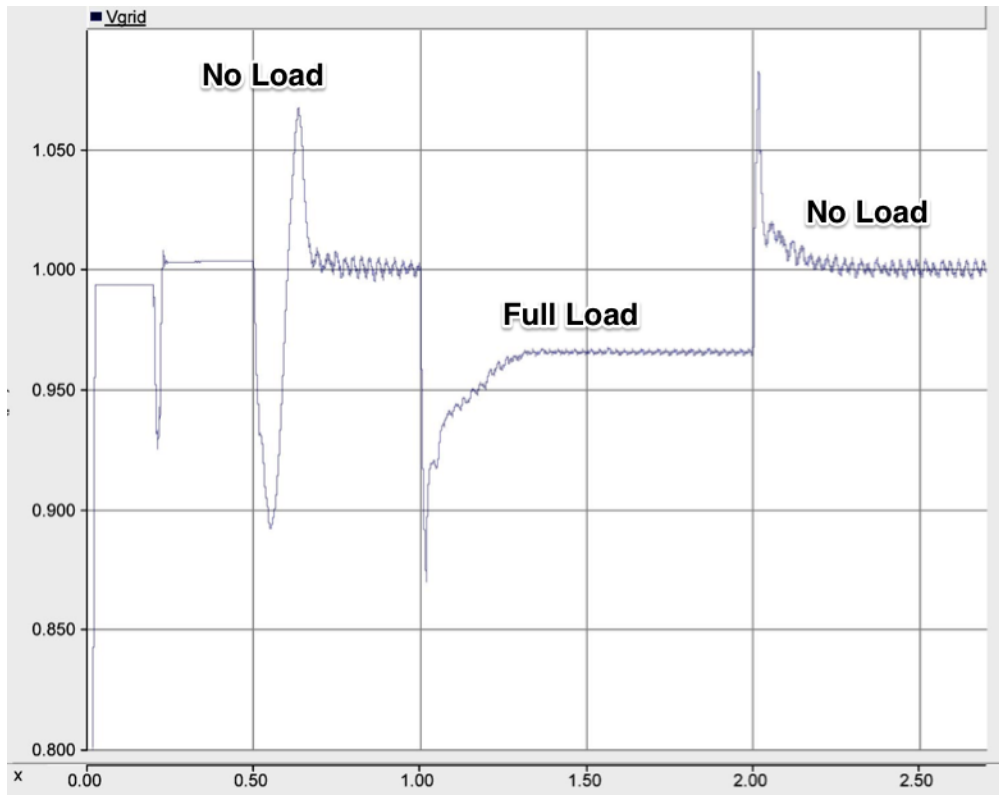


Figure 5.12 PCC Voltage, Synchronous Operation Without Parallel Rectifier

Another difference between the synchronous unit voltage profile and the single-unit voltage profile is the voltage response during a full-load condition. The single-unit voltage response is more rounded with no knee. The synchronous unit voltage response has two knee points: the first knee occurs at 1.08 seconds and is a result of the load resistance and reactance values stabilizing. The second knee occurs at 1.3 seconds and is a result of the dc voltage stabilizing to 2.0 kV. The difference in shape is due to the increased PCC voltage versus that of the single-unit test case. The larger PCC voltage causes the dc voltage regulator control system to behave slightly differently.

### 5.3.2 Synchronous Operation With Parallel Rectifier

This test characterizes the operation of both D-STATCOMs when they are brought online with no parallel rectifier. The results are shown in Table 5.7 and the PCC voltage profile is shown in Figure 5.13.

Table 5.7 Measured Values, Synchronous Operation With Parallel Rectifier

<b>PCC Steady State Full Load Voltage (pu)</b>	<b>Full Load Response Time (ms)</b>	<b>No Load Response Time (ms)</b>	<b>Full Load THD</b>	<b>No Load THD</b>
0.9647	329	235	1.53%	3.08%
<b>P supplied by D-STATCOM under full load(MW)</b>	<b>Q supplied by D-STATCOM under full load (Mvar)</b>	<b>Full load dc capacitor voltage (kV)</b>	<b>Inrush Current (kA)</b>	<b>dc voltage ripple (kV)</b>
-0.044	1.018	1.985	5.83	0.01

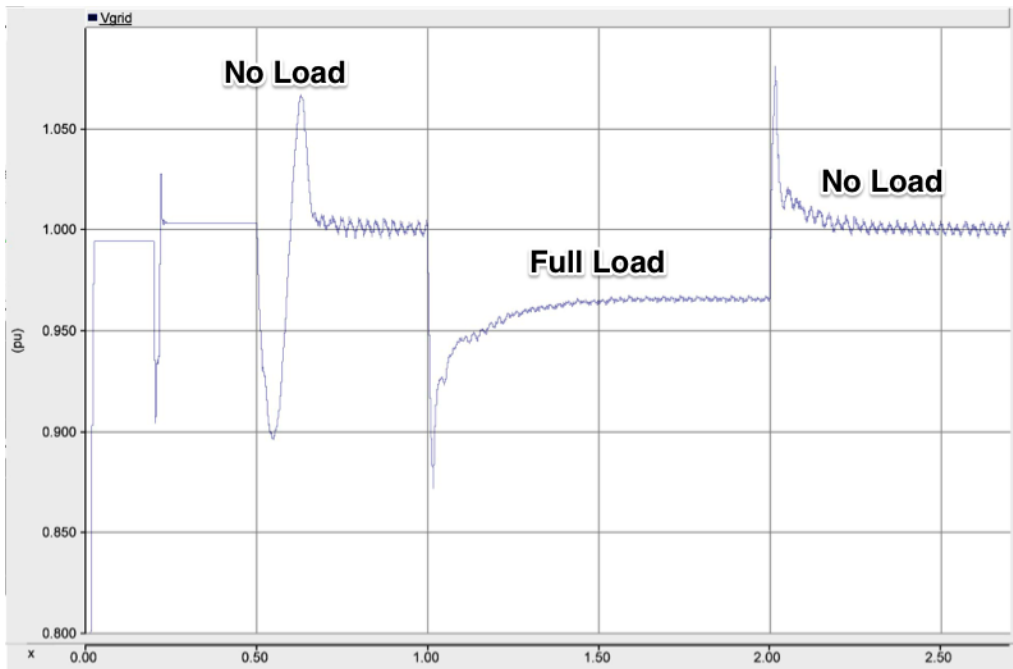


Figure 5.13 PCC Voltage, Synchronous Operation With Parallel Rectifier

Results are similar to those of synchronous operation without the parallel rectifier. The main difference between the results of the two test cases are the significantly larger inrush current of 5.83 kA found with synchronous operation with parallel rectifier.

The PCC inrush voltages for synchronous operation both with and without the parallel rectifier are plotted in Figure 5.14. The voltage profiles are similar to those of single-unit operation, but the voltage swings are larger since twice the effective capacitance is charging during that period.

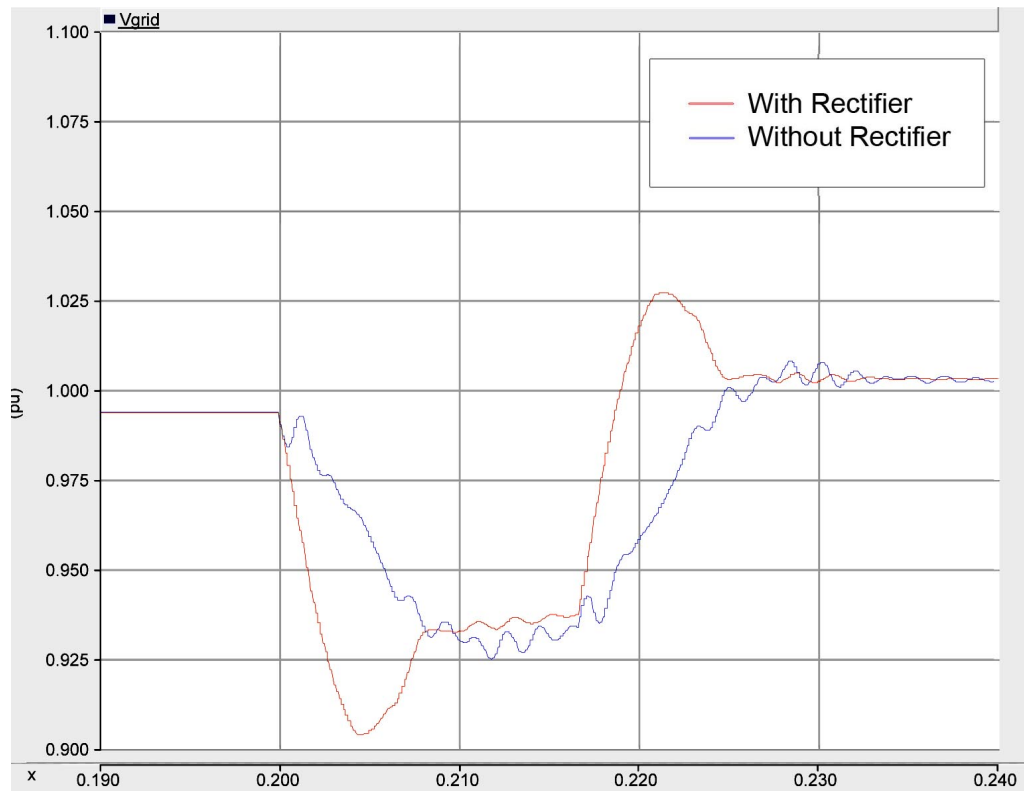


Figure 5.14 PCC Inrush Voltage, Synchronous Operation With and Without Parallel Rectifier

### 5.3.3 Synchronous Operation With Parallel Rectifier and Light Load

This test case is identical to the above test case, except the load is 1.2 MW + 0.75 Mvar. The purpose of this test is to analyze the performance of the system when the D-

STATCOMs are not pushed to supply 100% of their full rated reactive power. Because the modulation index of the ac voltage regulator is not forced to its high value of 1.0, this test case also reveals instability that may exist in the ac voltage regulator control system due to oscillation of the modulation index. Results for this test case are shown in Table 5.8 and the PCC voltage profile is shown in Figure 5.15.

Table 5.8 Measured Values, Synchronous Operation With Parallel Rectifier and Light Load

PCC Steady State Full Load Voltage (pu)	Full Load Response Time (ms)	No Load Response Time (ms)	Full Load THD	No Load THD
1.001	237	271	1.82%	3.07%

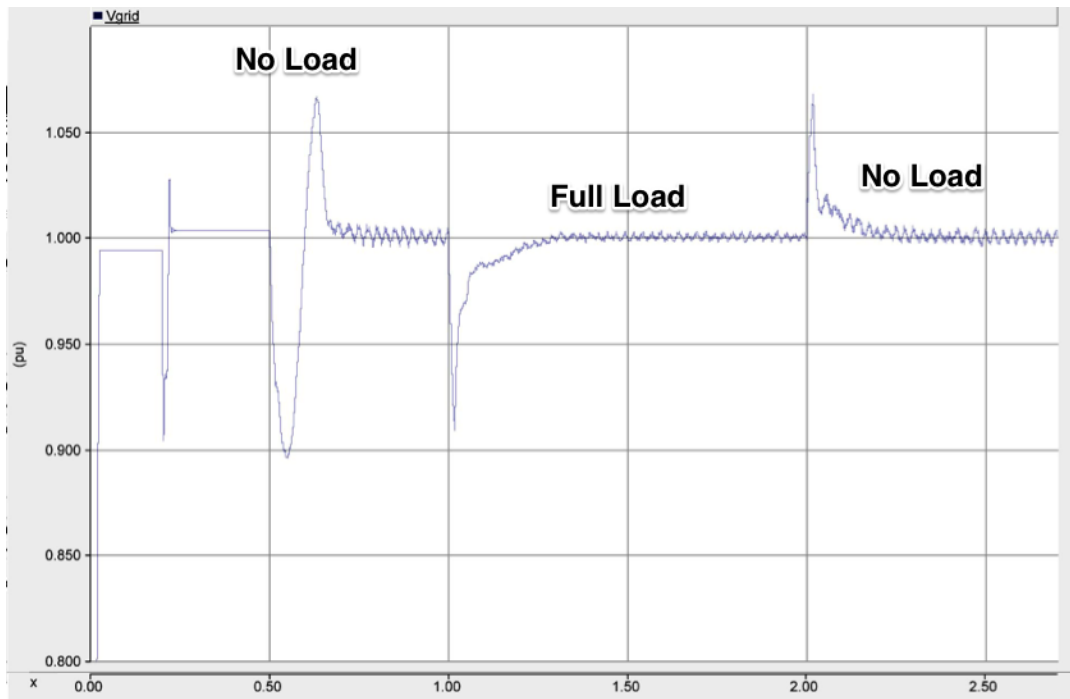


Figure 5.15 PCC Voltage, Synchronous Operation With Parallel Rectifier and Light Load

The full-load response time is faster for this case than in previous cases because the D-STATCOMs are not required to supply their full rated reactive power. The PCC voltage is brought up to its nominal value of 1.0 pu and remains stable. All other measured values of the test are consistent with previous test cases.

Overall the performance of dual synchronous D-STATCOMs is very similar to that of individual STATCOM operation. Notable differences include a higher full-load PCC voltage and larger voltage swings during the turn-on and capacitor charging periods. The system shows no signs of instability in these test cases, both for full load response and light load response. Furthermore, the parallel rectifier has a limited effect on all the test cases.

#### **5.4 Asynchronous D-STATCOM Operation**

For the asynchronous test case, both D-STATCOMs are connected to the PCC at different times and their respective inverters are also turned on at different times. The load is then connected to the PCC after both D-STATCOMs are operational. This test reveals any effect that the difference in turn-on time has on the stability and performance of the system.

For this test cases, both the load and the D-STATCOMs are disconnected from the PCC. At 0.2 seconds, the first D-STATCOM is connected to the PCC but its inverter remains off. At 0.4 seconds, the second D-STATCOM is connected to the PCC. At 1.0 second, the inverter of the first D-STATCOM is turned on. At 1.5 seconds, the inverter of the second D-STATCOM is turned on. At 2.0 seconds, the 1.7 MW + 1.0 Mvar load is connected to the PCC. At 3.0 seconds, the load is disconnected from the PCC.

Because the parallel rectifier only significantly affects initial charging performance of the dc capacitor, it is included in this test case. Performance is likely to be very similar without the parallel rectifier, so the parallel rectifier is included to maintain consistency with the initial model presented in [22].

Results for this test case are shown in Table 5.9 and a plot of the PCC voltage response is shown in Figure 5.16.

Table 5.9 Measured Values, Asynchronous D-STATCOM Operation With Full Load

PCC Steady State Full Load Voltage (pu)	Full Load Response Time (ms)	No Load Response Time (ms)	Full Load THD	No Load THD
0.965	328	284	1.53%	3.19%

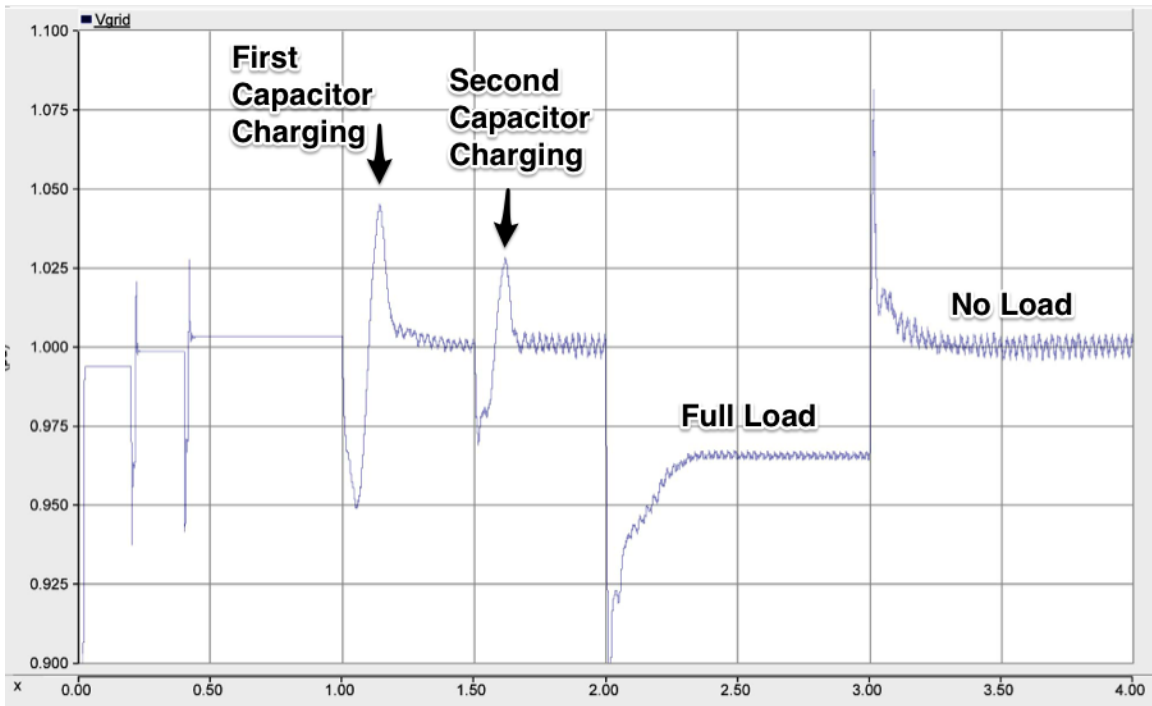


Figure 5.16 PCC Voltage, Asynchronous Operation With Full Load



Results for this test case share similarities with the results from synchronous operation, with the exception of initial turn-on characteristics. When the first D-STATCOM inverter is turned on, the voltage fluctuates from a low of 0.95 pu to a peak of 1.04 pu. This fluctuation is similar to the fluctuation seen in the single-unit operation test case. This is to be expected since there is only one D-STATCOM online when the first D-STATCOM is brought online. However, when the second D-STATCOM is brought online, the voltage fluctuation is significantly less, reaching a low point of 0.972 pu and a high of 1.027 pu. This is because the first D-STATCOM is able to supply reactive power to support the voltage of the PCC while the second dc capacitor is charging. A plot of real and reactive power transfer for both D-STATCOMs shows the action by which this occurs, as seen in Figure 5.17.

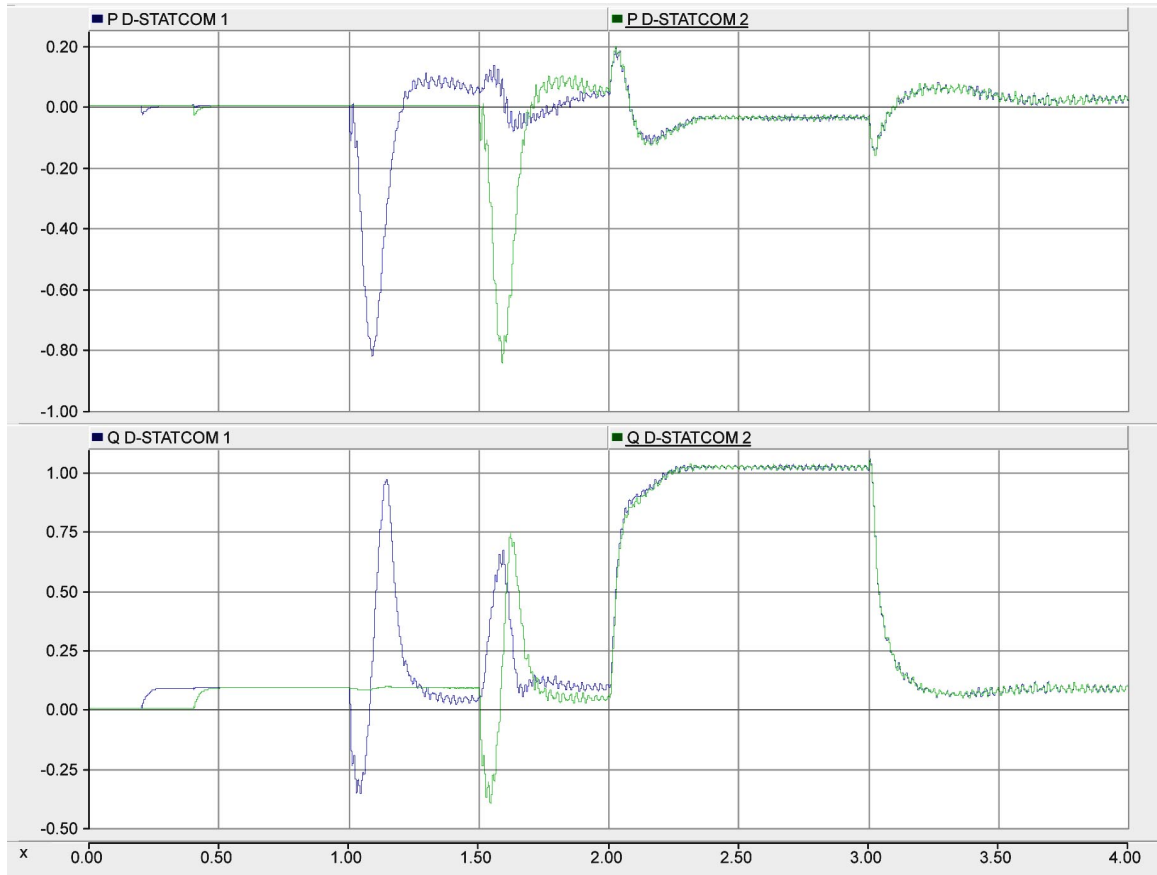


Figure 5.17 Real and Reactive Power Transfer, Asynchronous Operation With Full Load

As seen in Figure 5.17, each D-STATCOM draws significant real power during its initial charging phase. However, the D-STATCOM is unable to provide significant real power during steady state operating conditions, so the first D-STATCOM supplies a short burst of 0.7 Mvar to regulate the voltage of the PCC when the second D-STATCOM is turned on. Once both D-STATCOMs are turned on and their dc capacitors are fully charged, real and reactive power transfer are nearly identical for both units.

### 5.5 Asynchronous D-STATCOM Operation With Initial Load

For these test cases, the load is initially connected to the PCC while both D-STATCOMs remain offline. At 0.2 seconds, the first D-STATCOM is connected to the PCC, but its inverter remains off. At 0.4 seconds, the second D-STATCOM is connected

to the PCC. At 1.0 second, the first D-STATCOM is turned on. At 1.5 seconds, the second D-STATCOM is turned on. At 2.0 seconds, the load is turned off. As in the previous test case, the parallel rectifier is included in both of the following test cases.

The purpose of these test cases is to characterize the performance of the D-STATCOMs when they are required to simultaneously charge their respective dc capacitors while also regulating the voltage of the PCC when a load is already connected. These test cases, especially the full-load test case, represent some of the largest disturbances that this system may see since both the dc voltage error and the ac voltage error is initially high. Thus, stability during these test cases is an important indicator of the system's overall stability.

### 5.5.1 Asynchronous Operation with Full Initial Load

This test case uses the full initial load of 1.7 MW + 1.0 Mvar. Results are shown in Table 5.10 and the voltage profile of the PCC is plotted in Figure 5.18.

Table 5.10 Measured Values, Asynchronous Operation With Full Initial Load

<b>PCC Steady State Full Load Voltage (pu)</b>	<b>Full Load Response Time (ms)</b>	<b>No Load Response Time (ms)</b>	<b>Full Load THD</b>	<b>No Load THD</b>
0.9648	204	248	1.41%	3.18%

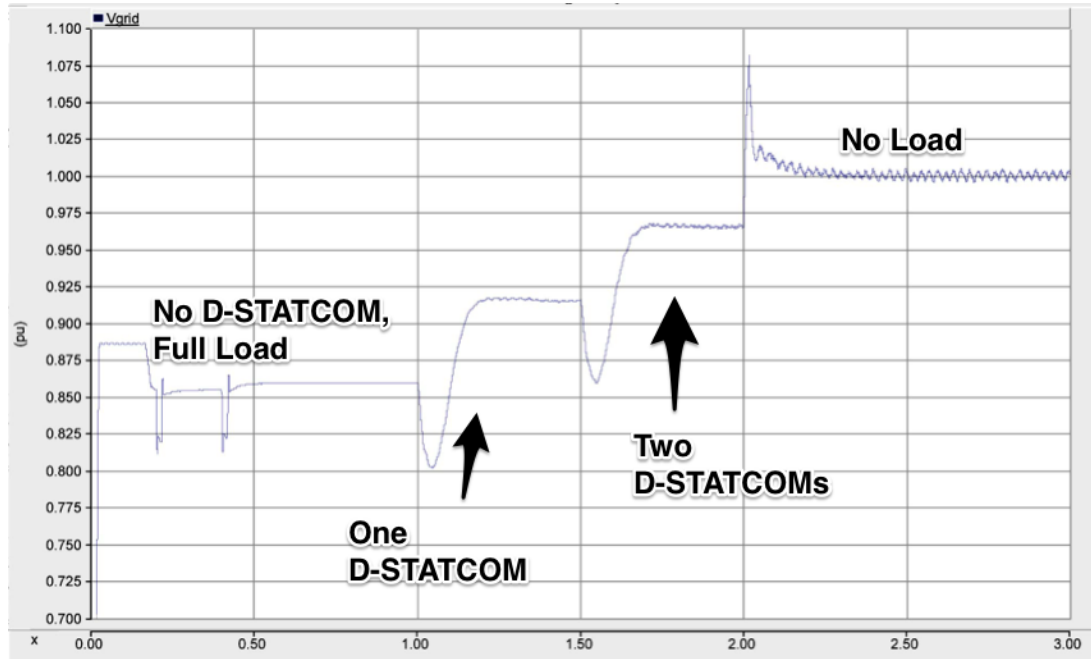


Figure 5.18 PCC Voltage, Asynchronous Operation With Full Initial Load

The response times, particularly the full-load response times, for this test case are among the best of all the test cases thus far. This can be explained by the tuning parameters selected for the dc and ac voltage regulators. Because the tuning parameters for both regulators are intended to strike a balance between initial charging performance and load response performance, these parameters are especially suited to this test case, where both charging and load response occur simultaneously.

As can be seen in Figure 5.18, when each D-STATCOM is turned on, the PCC voltage initially drops for about 50 ms while the dc capacitor charges to its nominal voltage. After that period, the PCC voltage quickly rises until each D-STATCOM produces full rated power. No-load response is the same as in previous test cases.

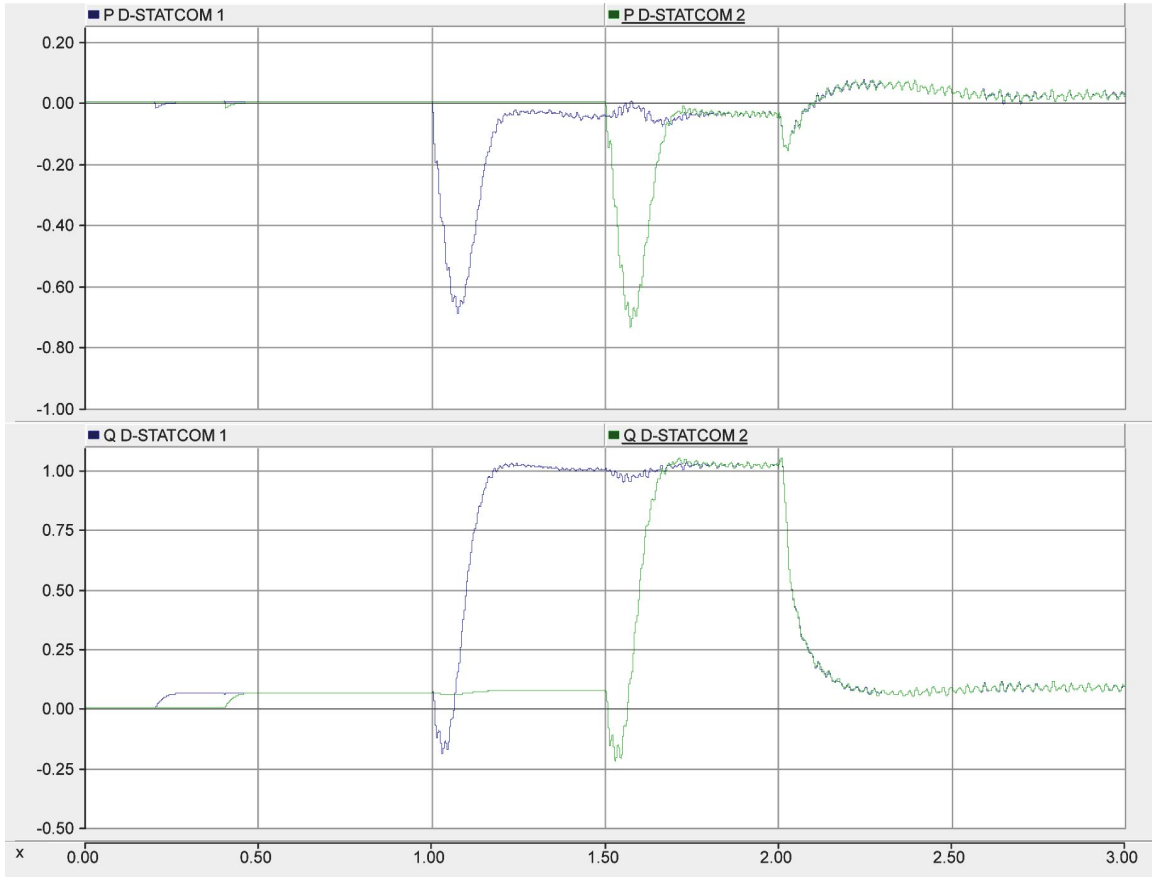


Figure 5.19 Real and Reactive Power Transfer, Asynchronous Operation With Full Initial Load

Figure 5.19 shows the real and reactive power transfer of both D-STATCOMs during this test case. As in previous test cases, the initial charging of the dc capacitor results in a brief period of real power flowing into the D-STATCOM. However, because both the dc voltage and the ac voltage are being regulated simultaneously, reactive power is supplied by each D-STATCOM as soon as real power transfer passes its peak magnitude. When real power transfer reaches its minimum magnitude, reactive power rises to the D-STATCOM's full rated output.

### 5.5.2 Asynchronous Operation With Light Initial Load

This test case is identical to the previous test case, except the load is 1.2 MW + 0.75 Mvar. The purpose of this test is to analyze the performance of the system when the D-STATCOMs are not pushed to supply 100% of their full rated reactive power. Results for this test case are shown in Table 5.11 and the voltage profile for the PCC is plotted in Figure 5.20.

Table 5.11 Measured Values, Asynchronous Operation With Light Load

PCC Steady State Full Load Voltage (pu)	Full Load Response Time (ms)	No Load Response Time (ms)	Full Load THD	No Load THD
0.9996	151	201	1.77%	3.07%

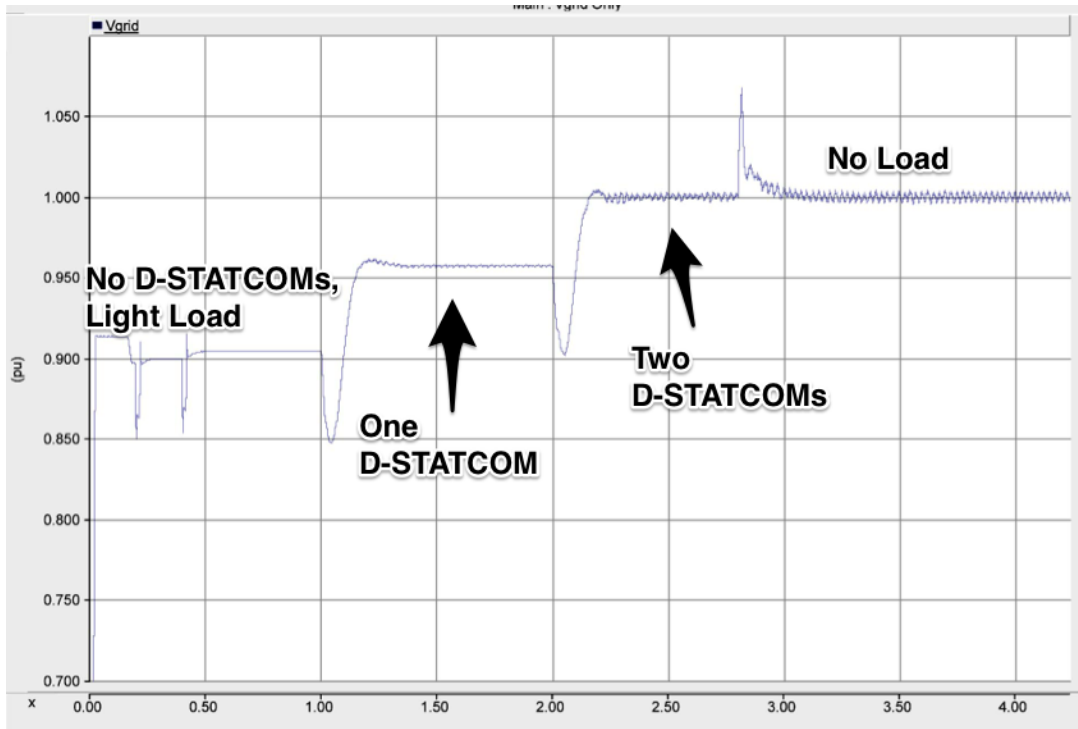


Figure 5.20 PCC Voltage, Asynchronous Operation With Light Initial Load

The response times for this test case are better than all previous test cases since the D-STATCOMs are not required to supply their full rated load when both units are operational. However, one D-STATCOM is unable to supply enough reactive power to bring the PCC voltage up to 1.00 pu. The real and reactive power transfer of both D-STATCOMs is shown in Figure 5.21.

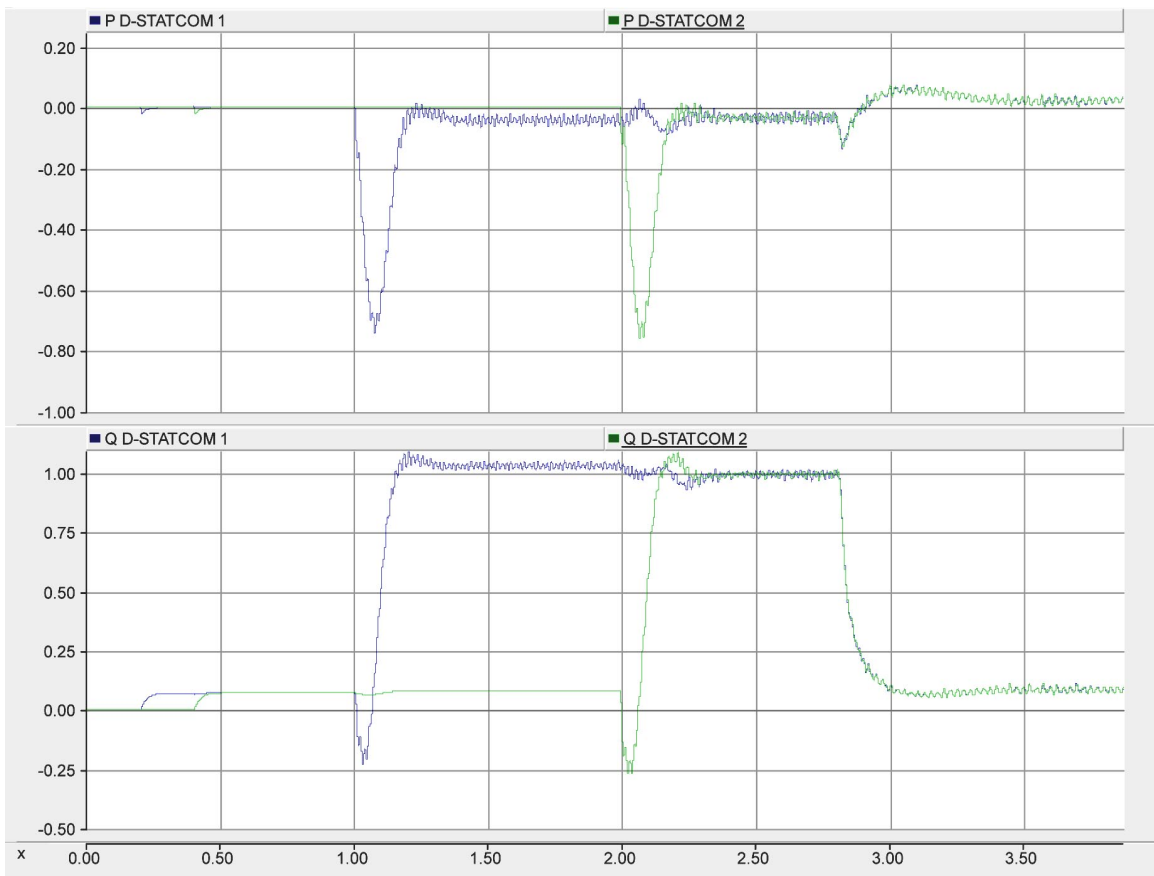


Figure 5.21 Real and Reactive Power Transfer, Asynchronous Operation With Light Initial Load

When the second D-STATCOM is turned on, it quickly overshoots to full reactive power output, causing the first D-STATCOM to slightly undershoot. The PCC voltage also experiences a slight voltage overshoot to 1.007 pu as a result of the change in reactive power supplied by the D-STATCOMs. Both D-STATCOMs recover to their

steady state reactive power output, which is slightly below their full rated reactive power. Despite the slight overshoot, the system remains stable and the reactive powers supplied by each D-STATCOMs converge to one value.

Overall, these two test conditions prove that this D-STATCOM model is capable of remaining stable when both D-STATCOMs are turned on at different times. The parallel rectifier has no negative effect on stability for these test cases, and both D-STATCOMs are able to converge on the correct reactive power output value to support the PCC voltage without significant fluctuations in reactive power transfer.



## 6 Conclusion

As our grid becomes increasingly stressed from higher demand and intermittent energy sources, newer techniques are being utilized to maintain the stability of our electrical infrastructure. The use of FACTS controllers has proven to be an effective strategy in quickly and precisely controlling power flow and regulating voltage in the grid. STATCOMs, in particular, are incredibly useful for regulating the grid voltage in response to quick changes in load, such as those encountered with intermittent renewable energy sources like solar photovoltaic systems. Their improved harmonic performance, their reduced size, and their desirable I-V characteristics make them superior to other shunt controllers such as SVCs.

The goal of this thesis was to characterize the performance of two D-STATCOMs operating on the same PCC. By using a variety of test scenarios that manipulate parameters such as load conditions and D-STATCOM turn-on sequence, comparisons can be drawn between single-unit operation and dual-unit operation, as well as operation both with and without the parallel full-wave rectifier.

This thesis demonstrates that operating two D-STATCOMs on the same PCC offer commensurate benefits compared to single-unit operation. Both units remain stable during a variety of operating conditions, including when both units are turned on asynchronously. Furthermore, the inclusion of parallel full-wave rectifiers has no significant effect on stability or reaction time. The parallel full-wave rectifiers also impose a significant power loss for the system. For these reasons, the parallel full-wave rectifier is an unnecessary expense to the system.

## **6.1 Future Work**

There are still a variety of ways that the performance of the D-STATCOM can be improved. Furthermore, there are also ways that D-STATCOMs can be integrated into existing equipment such as solar photovoltaic inverters. Two of these areas of further study are presented below.

### **6.1.1 Alternate Control Schemes for the DC and AC Voltage Regulators**

The control systems for this model are relatively simple. Both control systems use a PI topology with constant tuning coefficients. This resulted in a control system that strikes a compromise between turn-on stability and response time to load changes. One possible way to improve the performance of the D-STATCOMs is to implement adaptive tuning coefficients. For example, by using more relaxed coefficients during turn-on, inrush current could be reduced, resulting in a smaller voltage disturbance to the PCC. After the dc capacitor completes its initial charge, the coefficients could be changed to more aggressive values to improve the reaction time to changes in load.

### **6.1.2 Integration of D-STATCOM Capabilities into Grid-Tie Inverters**

The hardware of a D-STATCOM is nearly identical to that of a grid-tie inverter. One of the main differences between the two devices is the difference in controlling real and reactive power flow. By simply changing the control system of a grid-tie inverter and adding a dc capacitor, a grid-tie inverter could also act as a STATCOM. Such a system could supply real power when the sun is shining and supply reactive power when it is needed. Studies of such a system has already been done in [32] and [33], but such a configuration is not supported for grid-tie inverters that are not owned by utilities, per IEEE 1547 [34]. IEEE Std. 1547-2003 4.1.1 states that such a distributed resource cannot

be used to actively regulate the voltage at the PCC, which all but eliminates the use of a grid-tie inverter as a D-STATCOM. Further research must still be done to determine an effective and equitable way to integrate distributed resource voltage regulation into IEEE 1547. Such a solution must be safe for utility workers, easily controllable by system operators, and fair for both utilities and customers.

## Bibliography

- [1] Light-Duty Automotive Technology, Carbon Dioxide Emissions, and Fuel Economy Trends: 1975 Through 2013. Rep. United States Environmental Protection Agency, Dec. 2013. Web. 19 Feb. 2014.
- [2] Gelman, Rachel. *2012 Renewable Energy Data Book*. Rep. Ed. Mike Meshek. U.S. Department of Energy, Oct. 2013. Web. 17 Feb. 2014.
- [3] *2013 Key World Energy Statistics*. Publication. International Energy Agency, 2013. Web. 19 Feb. 2014.
- [4] "Electric Power Consumption (kWh per Capita)." *The World Bank*. Web. 19 Feb. 2014.
- [5] *Interim Report on the August 14, 2003 Blackout*. Rep. New York Independent System Operator, 8 Jan. 2004. Web. 17 Feb. 2014.
- [6] St. John, Jeff. "Cost of Big PV to the Grid: \$3 to \$8 per Megawatt-Hour." *Greentech Media*, 5 Jan. 2012. Web. 19 Feb. 2014.
- [7] Qingguang Yu; Pei Li; Wenhua Liu; Xiaorong Xie, "Overview of STATCOM technologies," *Electric Utility Deregulation, Restructuring and Power Technologies, 2004. (DRPT 2004). Proceedings of the 2004 IEEE International Conference on* , vol.2, no., pp.647,652 Vol.2, 5-8 April 2004
- [8] Taufik and D. Dolan, *Advanced Power Electronics*, 6 ed., San Luis Obispo, CA, 2013
- [9] Wamkeue, R., N. Kandil, J. East, and Y. Boisclair. *Series Compensation for a Hydro-Quebec Long Distribution Line*. Rep. Web. 23 Feb. 2014.
- [10] Glover, J. Duncan, Mulukutla S. Sarma, and Thomas J. Overbye. *Power System Analysis and Design*. 5th ed. Stamford: Cengage Learning, 2012. Print.

- [11] Harlow, James H. *Transformer Tapchanging Under Load: A Review of Concepts and Standards*. Proc. of 64th Annual Engineering Conference, Kansas City, MO.
- [12] Grande-Moran, Carlos, Ph.D. *Phase-shifting Transformer Modeling in PSS®E*. Rep. Siemens, Mar. 2012. Web. 1 Mar. 2014.
- [13] Uzochukwuamaka Okeke, T.; Zaher, R.G., "Flexible AC Transmission Systems (FACTS)," *New Concepts in Smart Cities: Fostering Public and Private Alliances (SmartMILE)*, 2013 International Conference on , vol., no., pp.1,4, 11-13 Dec. 2013
- [14] R. Grunbaum, A. Sannino, C. Wahlberg, "Use of FACTS for enhanced flexibility and efficiency in power transmission and distribution grids", ABB.
- [15] Singh, Bindeshwar, K.S. Verma, Pooja Mishra, Rashi Maheshwari, Utkarsha Srivastava, and Aanchal Baranwal. "Introduction to FACTS Controllers: A Technological Literature Survey." *International Journal of Automation and Power Engineering* 1.9 (2012): 193-221.
- [16] Raza, Mashhood, and Zain Zia. *Design and Simulation of Thyristor Controlled Series Capacitor*. Rep. Web. 03 Mar. 2014.
- [17] Kamarposhti, Mehrdad A., and Mostafa Alinezhad. *Comparison of SVC and STATCOM in Static Voltage Stability Margin Enhancement*. Rep. World Academy of Science, Engineering and Technology, 2009. Web. 2 Mar. 2014.
- [18] ABB. *SVC Static Var Compensator An Insurance for Improved Grid System Stability and Reliability*. Västerås, Sweden: ABB, 2010.
- [19] Adepoju, G.A., and O.A. Komolafe. "Analysis and Modeling of Static Synchronous Compensator (STATCOM): A Comparison of Power Injection and Current Injection Models in Power Flow Study." *International Journal of Advanced Science and Technology* 36 (2011): 65-75.

- [20] Ravi Kumar, S.V., and S. Siva Nagaraju. "SIMULATION OF D-STATCOM AND DVR IN POWER SYSTEMS." *ARPJ Journal of Engineering and Applied Sciences* 2.3 (2007): 7-13.
- [21] Roy, Tamal, and Mahesh Singh. "PSCAD Simulation Model of D-Statcom for Voltage Sag Improvement." *International Journal of Computer Applications* 59.2 (2012): 45-48.
- [22] Taufik. "DVC Model & Study," unpublished.
- [23] "Real Time Digital Simulator." *Center for Advanced Power Systems*. Florida State University, n.d. Web. 20 Mar. 2014.
- [24] "Diamond Years: 1990 - 2000." *Diamond Years*. APEGM, n.d. Web. 20 Mar. 2014.
- [25] IEEE Recommended Practices and Requirements for Harmonic Control in Electrical Power Systems," *IEEE Std 519-1992* , vol., no., pp.1,112, April 9 1993
- [26] American National Standard Preferred Voltage Ratings for Electric Power Systems and Equipment (60 Hz)
- [27] ANSI C84.1-1989.
- [28] Heathcote, Martin. *J & P Transformer Book*. 13th ed. Amsterdam: Elsevier, 2007. Print.
- [29] Knapczyk, Michał, and Krzysztof Pienkowski. *Analysis of Pulse Width Modulation Techniques for AC/DC Line-Side Converters*. Rep.
- [30] IXYS Corporation, Appl. Note IXAN0063, p. 1.
- [31] Zare, Firuz. "EMI Issues in Modern Power Electronic Systems." *IEEE EMC Society Newsletter* 211 (Spring 2009): 69. Print.
- [32] Johnson, Benjamin. *MODELING AND ANALYSIS OF A PV GRID-TIED SMART INVERTER'S SUPPORT FUNCTIONS*. Thesis. California Polytechnic State University, 2013.
- [33] Varma, R.K.; Das, B.; Axente, I.; Vanderheide, T., "Optimal 24-hr utilization of a PV solar system as STATCOM (PV-STATCOM) in a distribution network," *Power*

*and Energy Society General Meeting, 2011 IEEE* , vol., no., pp.1,8, 24-29 July 2011

- [34] IEEE Application Guide for IEEE Std 1547(TM), IEEE Standard for Interconnecting Distributed Resources with Electric Power Systems," *IEEE Std 1547.2-2008* , vol., no., pp.1,217, April 15 2009